A model for how fission yeast cells scale their size with ploidy

Ichiro Yamashita

Center for Gene Science, Hiroshima University, Kagamiyama 1-4-2, Higashihiroshima 739-8527, Japan.

Correspondence: iyama@hiroshima-u.ac.jp
Ichiro Yamashita https://orcid.org/0000-0001-6016-5438

ABSTRACT

It has long been known that eukaryotic cells with more DNA content are larger in cell size. However, no molecular mechanisms for this universal rule have been given. In the fission yeast *Schizosaccharomyces pombe*, diploid cells grow faster at 1.5-fold rate than haploid cells during the same cycle time. Here I discovered that cell division genes control not only cell growth or cell extension rate (CER) but also cycle time dose-dependently in diploid cells. These genes are well-known regulators for Cdc2, a conserved master regulator of eukaryotic cell cycle, such as inhibitors (*wee1*$^+$ and *pom1*$^+$) and activators (*cdc25*$^+$ and *nim1*$^+$). Actin content and its dynamics between monomer and polymer forms also control CER and cycle time through nuclear accumulation of Wee1 and Cdc25. Remarkably, doubling these genes in haploids reproduced CER of diploids. I propose a model in which regulatory cascades for Cdc2 activity govern the cell-size scaling with ploidy.

KEYWORDS

actin, *cdc25*, *nim1*, ploidy, scaling, *wee1*

Introduction

The general association between DNA content and cell size has long been recognized in unicellular eukaryotes, plants, and animals [1-3]. Polyploid cells with multiple copies of chromosome sets occur frequently in the development and differentiation of plants and animals, and large polyploid cells are crucial to morphology, metabolism, and tissue-

specific function [4,5]. However, no mechanisms explaining this universal rule for cell size determination have been demonstrated. Here I used the fission yeast and explored the possibility for the involvement of cell division genes that control cyclin-dependent protein kinase, Cdc2 [6]: *cdc13*$^{+}$ (cyclin) [7], *wee1*$^{+}$ (an inhibitory protein kinase) [8], *cdc25*$^{+}$ (an activating protein phosphatase with antagonistic action to Wee1) [9], *nim1*$^{+}$/*cdr1*$^{+}$ kinase (inducer of mitosis by inhibiting Wee1) [10,11], and its upstream inhibitory effectors, *pom1*$^{+}$ [12] and *nif1*$^{+}$ [13]. I also examined whether *act1*$^{+}$ (actin) [14] is involved in cell-size control because actin cables are thought to serve as tracks for secretory vesicle transport to the tip [15-17].

Cdc2 is a conserved key regulator for entry into mitosis and its activity is thought to be critical to cell-size determination [18]. Loss of Wee1 activity induces premature activation of Cdc2 and therefor causes cells to enter mitosis before sufficient growth has occurred, producing two abnormally small daughter cells. Similarly, mutants with lower Cdc2 activity (such as *cdc2*$^{-}$, *cdc13*$^{-}$, and *cdc25*$^{-}$) undergo delayed entry into mitosis, producing abnormally large cells. However, these genetic analyses overlook the possibility that Cdc2 controls growth rate during G2 period. Throughout this work, I measured growth rate as a major determinant of cell-size scaling with ploidy because diploid cells grow faster than haploid cells during the same doubling time in fission yeast [19] as well as in budding yeast [20]. By using diploid and tetraploid cultivars of ryegrass, Sugiyama demonstrated that polyploidy increases leaf size mainly by increasing the cell elongation rate without significant differences in cell division parameters [21]. Zhou et al. also reported that tetraploid crucian carp cells grow bigger than diploid cells without affecting proliferation (or cell division) [22]. Collectively, these results may lead to a generalization that polyploid cells scale their size or volume by controlling growth rate.

The aim of my investigation was to search for mechanisms by which cell division genes control Cdc2 activity and growth rate dose-dependently during G2. I propose systems level control of Cdc2 as a critical regulator of growth rate, in which limited number of cell division genes may account for the cell-size scaling with ploidy.

Materials & methods

Strains

The *S. pombe* strains used in the experiment are listed in Supplemental Table 1. The strains bearing mutant alleles (*cdc2-L7*, *cdc2-3w*, *cdc25-22*, *cdc13-117*, and *wee1-50*) or deletions (*cdc25Δ::ura4*$^{+}$, *wee1Δ::ura4*$^{+}$, and *nim1Δ::LEU2*) were gifts from P. Russell and P. Nurse [8-10,23]. A strain bearing *pom1Δ::ura4*$^{+}$ was from J. Bähler and J. R.

Pringle [12]. A strain bearing *cps8-188* and a plasmid carrying *act1*$^+$ were from J. Ishiguro [14]. Strains bearing *cdc25Δ::ura4*$^+$*::cdc25-GFP::leu1*$^+$ and *cdc25Δ::ura4*$^+$*::cdc25-NLS-GFP::leu1*$^+$ were from P. G. Young [24]. Strains bearing *wee1Δ::ura4*$^+$ and either *lys1*$^+$*::GFP-wee1* or *lys1*$^+$*::GFP-NESx2-wee1* were from H. Masuda [25]. Strains bearing deletions of *act1Δ::ura4*$^+$ [14], *cdc13Δ::ura4*$^+$ [7], and *nif1Δ::ura4*$^+$ [13] were constructed as described previously by the one-step gene disruption method [26]. Strains bearing two copies of *act1*$^+$ (2x*act1*$^+$*::ura4*$^+$), *cdc13*$^+$ (2x*cdc13*$^+$*::ura4*$^+$), *cdc25*$^+$ (2x*cdc25*$^+$*::ura4*$^+$), *nim1*$^+$ (2x*nim1*$^+$*::ura4*$^+$), and *pom1*$^+$ (2x*pom1*$^+$*::ura4*$^+$) were constructed by insertion into native loci of pBR322-based plasmids carrying *ura4*$^+$ and the respective genes (6.5-kb *Eco*RI-*Hin*dIII fragment of *act1*$^+$, 4.6-kb *Pvu*II-*Bam*HI fragment of *cdc13*$^+$, 5.2-kb *Sph*I-*Pvu*II fragment of *cdc25*$^+$, 3.3-kb *Bam*HI-*Eco*RI fragment of *nim1*$^+$, and 6.5-kb *Nhe*I-*Sph*I fragment of *pom1*$^+$) after linearization by digestion within coding regions with *Bam*HI, *Xho*I, *Bam*HI, *Xho*I, and *Bgl*II, respectively. Plasmids carrying *cdc13*$^+$, *cdc25*$^+$, *nif1*$^+$, *nim1*$^+$, and *pom1*$^+$ and an *adf1-1* strain were provided by the National Bio-Resource Project (NBRP), Japan.

Standard procedures were used for cell culture and genetic manipulations [27]. Diploid cells were constructed by isolation of prototrophic cells after crossing haploid cells with opposite mating type (h$^+$ or h$^-$), each bearing *ade6-M210* or *ade6-M216*. Diploid cells were also selected after cultivation of haploid cells on YES plates containing phloxin-B. Diploid cells homozygous for mating type (h$^{+/+}$ and h$^{-/-}$) were isolated by manipulator after repeated (usually 2 or 3 times) cultivation of h$^{+/-}$ diploid on EMM2 plates at 28℃ for 2 days. Diploid cells heterozygous for two or three deletions (marked with *ura4*$^+$) were selected after tetrad dissection of asci from tetraploid cells made by mating between h$^{+/+}$ and h$^{-/-}$ diploids, each heterozygous for one or two deletions. Diploids heterozygous for two or three deletions were verified by tetrad analysis after crossing with tester diploids bearing *ura4-D18*/*ura4-D18*, in which Ura$^+$ segregants appear in a manner of PD : NPD : T = 1 : 1: 4 from the cross with the diploid heterozygous for two deletions or in a manner of (2 Ura$^+$: 2 Ura$^-$) : (3 Ura$^+$: 1 Ura$^-$) : (4 Ura$^+$: 0 Ura$^-$) = 1 : 16: 19 from the cross with the diploid heterozygous for three deletions. Haploids bearing two or three loci of two copies of genes (marked with *ura4*$^+$) were also verified by tetrad analysis after crossing with tester haploids bearing *ura4-D18*, in which Ura$^+$ segregants appear as above. Haploids bearing four or five loci of two copies of genes were verified by tetrad analysis after back-crossing with haploids bearing three or four loci of two copies of genes, respectively, in which tetrads were segregated as 2 (longer cells) : 2 (shorter cells).

Measurement of CER

Cells were grown exponentially in EMM2 for 24 h to a maximum density of 5 x 10^6 cells/ml before the initiation of all experiments. Temperature-sensitive cells were cultured at 28℃, and other cells were grown at 28℃ or 36.5℃ as indicated. Before measurement of CER, more than three strains with the same genotype were measured for length of long axes of more than 100 cells with septum. Strains having the closest match to average cell length of genotype were chosen for measurement of CER. Aliquot of culture was collected by centrifugation for 30 sec, resuspended and spread on thin EMM2 agar plates. A block (15 x 15 mm) was cut and set upside down on a glass-base dish (diameter, 35 mm; code 3970-035, Iwaki, Japan). The dish was sealed by parafilm and set on a thermo plate (MATS-55RAF20, Tokai Hit, Japan) on inverted microscope (Nikon Eclipse TE2000-U). The dish was fastened with cellotape on the thermo plate, and finally covered by a plastic petri dish (diameter, 85 mm) for temperature control. The temperature on the agar was checked with a contact thermistor in trial experiments, and kept at 28℃ or 36.5℃ as indicated. Room temperature was controlled by air conditioner more than 10℃ lower than the temperature of the agar. Cells were visualized under x40 magnification, and photographed every 30 min for 6 to 10 h depending on doubling time of strains. Images were acquired with a digital CCD camera (C4742-95-12ERG, Hamamatsu Photonics) and processed using HCImage Live U11158-01 software (Hamamatsu Photonics). Long axes of cells were measured during the first and the second divisions. The average cell-length values of 50 to 70 individual cells were plotted against time axis, and CER was calculated every 30 min. For determination of CER of temperature-sensitive strains, cells were precultured at 36.5℃ for 30 min on agar film and photographed every 30 min. For *cdc25-22*, *cdc2-L7*, and *cdc13-117* cells, average cell length of individual cells in the same field was calculated and plotted against incubation time, from which CER was calculated. A minor population of cells that divided within 3 h after the temperature shift was omitted. For *act1-ts* or *adf1-1* cells, cell length of individual cells was measured until cell lysis and plotted against incubation time, and maximum growth rate of individual cells was used as estimate of growth rate against initial cell length at the temperature shift. Cell length and CER are presented by average with standard deviation (SD). Statistical significance was tested by student's two-sided *t*-test. *P* values are presented as follows: *, <0.05; **, <0.001; ***, <0.0001; and n.s., not significant.

Fluorescence microscopy

Cells were grown exponentially at 28℃. In most experiments, exponential cells grown at 28℃ were shifted to 36.5℃ for further incubation as indicated. Cells were visualized under x40 or x100 oil magnification using the same microscopy set as above with a GFP filter. Number of cells showing nuclear localization (not uniform distribution in both nucleus and cytoplasm) of GFP signal was scored. Nuclear localization for each genotype was estimated as an average of more than three independent strains with SD. Total content and intensity of GFP signal in the nuclei were measured by manually surrounding the nuclei and processing using the same software as above. Values are presented by average (arbitrary unit) with SD. Statistical significance was as described above.

Results

Diploid cells grow faster than haploid cells

The previous study reported, by measuring cell length of individual cells at birth and septation from time-lapse films, that diploid cells grow faster than haploid cells during the same cycle time [19]. I began my inquiry by measuring CER of haploid and diploid cells throughout the cell cycle. For this purpose, cells were pre-cultured exponentially in EMM2 at 28℃, spread on EMM2 agar film, and incubated at the same temperature. Cell growth was monitored by taking photos of cells on the agar film every 30 min between one division and the next (Figure 1(a)) and by measuring long axis of *S. pombe* cells, because they grow only by tip extension. CER was calculated in every 30 min from average cell length of 65 cells (Figure 1(b)). This analysis clearly indicated that diploid cells grow faster than haploid cells at about 1.5-fold rate until arrest of extension near the septation stage in the cell division cycle.

Cell division genes control cell growth

To explore whether cell division genes are involved in growth control, temperature-sensitive mutations that affect Cdc2 activity were examined. For this purpose, cells were pre-cultured exponentially at a permissive temperature (28℃), spread on EMM2 agar film, and incubated at a restrictive temperature (36.5℃). Mutations that abolish Cdc2 activity such as *cdc25-22*, *cdc2-L7*, and *cdc13-117* caused longer cells than wild-type (not shown) and increased CER in both haploid and diploid ($p<0.0001$, maximum CER compared between wild and mutant) (Figure 2). On the contrary, *wee1-50* giving higher Cdc2 activity decreased CER of both haploid and diploid ($p<0.0001$) (Figures 2). These results indicate that Cdc2 activity controls CER negatively.

Haplo-insufficient roles of cell division genes

If cell division genes were involved in ploidy-dependent growth control, deletion of one of two copies of them in diploid would affect CER. To explore this idea, heterozygotes (*cdc25Δ*/+, *wee1Δ*/+, or *act1Δ*/+) were examined for growth kinetics (Figure 3(a)) and CER (Figure 3(b)). All heterozygotes grew more slowly than parental diploid, indicating haplo-insufficient positive roles of $cdc25^{+}$, $wee1^{+}$, and $act1^{+}$. The *cdc25Δ*/+ cells extended cycle time and were finally longer at septation stage than wild-type cells. The *wee1Δ*/+ cells showed an equivalent CER to haploid control, but grew for a longer time as well as the *wee1Δ*/*wee1Δ* cells used as a reference. The *act1Δ*/+ cells, in which actin polymers were considerably reduced (Supplemental Figure 1), slowed down CER appreciably later in the cycle and underwent premature septation before relatively delayed cell separation.

To investigate genetic epistatic relationship, double heterozygotes harboring *wee1Δ*/+ (*wee1Δ*/+ *cdc25Δ*/+ and *wee1Δ*/+ *act1Δ*/+) were examined (Figure 3(b)). Compared with the *wee1Δ*/+ single heterozygote, they showed no reduction or indeed slight elevation of CER. Conversely, *wee1Δ*/+ reduced CER of *cdc25Δ*/+ and *act1Δ*/+ heterozygotes. These results indicate that *wee1Δ*/+ is epistatic to *cdc25Δ*/+ and *act1Δ*/+ and suggest that positive roles of Cdc25 and Act1 (actin) work in the presence of sufficient amount of Wee1. Next, to investigate relationship between *cdc25Δ*/+ and *act1Δ*/+, double heterozygote (*cdc25Δ*/+ *act1Δ*/+) was compared with single heterozygotes (*cdc25Δ*/+ and *act1Δ*/+), resulting in similar CER in both cases (Figure 3(b)). This suggests that Cdc25 and Act1 function positively in the presence of sufficient amount of actin and Cdc25, respectively. I also examined the triple heterozygote (*wee1Δ*/+ *cdc25Δ*/+ *act1Δ*/+). CER of the strain was elevated compared with the double heterozygotes of *wee1Δ*/+ *cdc25Δ*/+ and *wee1Δ*/+ *act1Δ*/+ (Figure 3(b)), confirming negative roles of actin and Cdc25. The triple heterozygote showed similar CER to the *cdc25Δ*/+ *act1Δ*/+ heterozygote (Figure 3(b)), indicating that positive role of Wee1 depends on dosage of Cdc25 and actin. Together, I conclude that actin, Cdc25, and Wee1 execute positive roles interdependently and that actin and Cdc25 also act negatively under a Wee1-insufficient condition. Considering that Cdc2 is known to be involved in actin dynamics: actin filaments develop well or poorly in cells with lower or higher Cdc2 activity, respectively (Supplemental Figure 1) [16,28-30], I set up a hypothetical pathway that may explain the above genetic hierarchy (Figure 3(c)).

Cdc2 and actin dynamics control nuclear localization of GFP-Wee1

Since the genetic analysis predicted that Cdc25 and Act1 stimulate CER under the presence of sufficient amount of Wee1, together with my observation that longer cells

have more contents of nuclear GFP-Wee1 in the cell cycle (Supplemental Figure 2), I supposed that Cdc2 activity and actin dynamics would control cellular behavior of Wee1. For this purpose, I examined whether several mutations affecting Cdc2 activity or actin dynamics as follows could affect intracellular behavior of GFP-Wee1: *cdc2-3w* (giving higher Cdc2 activity), *cdc2-L7*, *cdc25-22*, *cdc13-117* (severe reduction of Cdc2 activity), and two counteracting temperature-sensitive mutations affecting actin dynamics: *cps8-188* [14], wild type of which encodes actin itself, makes the mutant actin filament collapse to a significant extent at restrictive temperature (hereafter called *act1-ts*); and *adf1-1* [31], wild type of which encodes actin-depolymerizing factor/cofilin that promotes dissociation of monomers from the filament, disrupts actin dynamics and makes mutant cells depleted of monomers. I observed an increase both in nuclear localization (Figure 4(a)) and nuclear content (Supplemental Figure 3) of GFP-Wee1 in both haploid and diploid cells harboring *cdc2-3w* cells, in contrast, reduced nuclear localization of GFP-Wee1 in *cdc2-L7*, *cdc25-22*, and *cdc13-117* cells regardless of ploidy (Figure 4(a)). Furthermore, heterozygotes for either *cdc25Δ* (Figures 4(b)) or *cdc13Δ* (Figures 4(a)) also showed reduced nuclear localization. These results suggest that Cdc2 activity controls nuclear localization of GFP-Wee1 in both haploid and diploid, and that two copies of $cdc25^{+}$ or $cdc13^{+}$ are required to keep GFP-Wee1 in the nuclei of diploid cells. Next, I observed that *act1-ts* elevated nuclear content of GFP-Wee1 (Figure 4(c)), suggesting that increased amounts of actin monomers account for nuclear accumulation of GFP-Wee1. In favor with this result, the *adf1-1/adf1-1* diploid cells decreased nuclear content of GFP-Wee1 (Figure 4(c)), which was suppressed by *act1-ts/act1-ts* (Figure 4(a)). I also found that *act1Δ*/+ heterozygote showed reduced nuclear content of GFP-Wee1 (Figures 4(b)), indicating that one copy of $act1^{+}$ in diploid is not enough to accumulate GFP-Wee1 in the nucleus. Furthermore, the 3x$act1^{+}$ and *act1-ts*/*act1-ts* suppressed the reduced nuclear content of GFP-Wee1 in the *cdc25Δ*/+ or *cdc13Δ*/+ heterozygote and the *cdc13-117*/*cdc13-117* diploid, respectively (Figure 4(a)). Conversely, the *adf1-1*/*adf1-1* suppressed the increased nuclear accumulation of GFP-Wee1 in the *cdc2-3w*/*cdc2-3w* cells (Figure 4(a)). Together, these results reveal a specific role of actin monomer (or short actin oligomer) in the nuclear accumulation of GFP-Wee1 in diploid and suggest that Cdc2 controls nuclear localization of GFP-Wee1 through modulation of actin dynamics. These controls may be associated with nucleo-cytoplasmic transport system because GFP-NESx2-wee1, a version of GFP-Wee1 tagged with two copies of *n*uclear *e*xport *s*ignal [25], was mostly localized around the nuclear periphery with some in the nucleus and the cytoplasm regardless of temperature, ploidy, and mutations of cell division genes including *act1-ts*, *adf1-1*, and 3x$act1^{+}$ (Supplemental Figure 3 and data not shown).

However, actin dynamics play no or limited role in haploid because no apparent effect was found in the *act1-ts* and *adf1-1* haploids (Figure 4(a)).

Cdc2 and actin dynamics control nuclear localization of Cdc25-GFP

Next, I searched for possible relation of nuclear localization of Cdc25-GFP to Cdc2 activity and actin dynamics, since nuclear content of Cdc25-GFP increases with cell size (Supplemental Figure 2). I first examined whether mutational modulation of Cdc2 activity could affect nuclear localization of Cdc25-GFP by using mutant cells with higher (*wee1-50*) or severely reduced (*cdc13-117*) Cdc2 activity. I observed reduced nuclear localization by the *wee1-50* mutation regardless of ploidy (Figure 5(a)), however, constant nuclear localization of Cdc25-NLS-GFP (a version of Cdc25-GFP fused with a *n*uclear *l*ocalization *s*ignal) (Figure 5(a)), suggesting a specific role in nuclear transport. I also examined the effect of *wee1 Δ*/+, resulting in reduction of nuclear content of Cdc25-GFP (Figure 5(b)) but constant nuclear localization of Cdc25-NLS-GFP (Figure 5(a)). Conversely, *cdc13-117* cells accumulated nuclear Cdc25-GFP more abundantly irrespective of ploidy (Figure 5(a)). These results indicate that nuclear localization of Cdc25-GFP is associated with Cdc2 activity.

Next, I searched for control of nuclear localization of Cdc25-GFP through actin dynamics. To test this, I first used latrunculin A, a chemical reagent that destabilizes actin filament [32]. I found uniform cellular distribution of Cdc25-GFP but constant nuclear localization of Cdc25-NLS-GFP (Supplemental Figure 4), suggesting a specific role of actin dynamics in nuclear localization of Cdc25-GFP. I next used two counteracting temperature-sensitive mutations for actin dynamics, *act1-ts* and *adf1-1*. I observed that both *act1-ts* and *adf1-1* mutations greatly decreased nuclear accumulation of Cdc25-GFP irrespective of ploidy, but did not affect nuclear localization of Cdc25-NLS-GFP (Figure 5(a)). The *adf1-1* mutation was also effective in both *cdc13-117* haploid and *cdc13-117/cdc13-117* diploid (Figure 5(a)), in which otherwise Cdc25-GFP accumulates in the nuclei more abundantly than in wild-type cells (Figure 5(a)), revealing an active role of actin dynamics in the nuclear localization of Cdc25-GFP. However, I observed that *act1-ts* decreased nuclear localization of Cdc25-GFP in *cdc13-117/cdc13-117* diploid (Figure 5(c)) but did not in *cdc13-117* haploid (Figure 5(a)), suggesting more active roles of actin in diploid than in haploid. I also examined the effect of *act1Δ*/+, resulting in reduced nuclear content of Cdc25-GFP (Figure 5(b)). This indicates that one copy of $act1^{+}$ in diploid is not enough to accumulate Cdc25-GFP in the nucleus.

Positive roles of Cdc25 both in CER and division timing

I postulated that the reduced nuclear content of Cdc25-GFP accounts for both the decrease in CER and the elongated cycle time in the heterozygote harboring *wee1Δ*/+. To test this, I constructed *wee1Δ*/+ diploids harboring *cdc25-NLS-GFP*/*cdc25-NLS-GFP* for forced expression of Cdc25 in the nucleus as well as haploid and diploid controls (1n *cdc25-NLS-GFP* and 2n *cdc25-NLS-GFP*/*cdc25-NLS-GFP*, respectively). I observed that both controls showed ploidy-dependent growth kinetics and CER like the *cdc25-GFP* background albeit slower ones (Figure 6). However, the *wee1Δ*/+ diploids harboring *cdc25-NLS-GFP*/*cdc25-NLS-GFP* elevated CER and simultaneously recovered the delayed cycle time compared with the *wee1Δ*/+ diploids harboring *cdc25-GFP*/*cdc25-GFP* (Figure 6). These results suggest that nuclear accumulation of Cdc25 could act positively both for CER and cycle time at least under the Wee1-insufficient condition. These observations agree with my proposal that Cdc25 acts as a positive regulator for cell extension during G2 and are consistent with the previous conclusion that Cdc25 constitutes a key molecule in the auto-regulatory loop for acute activation of Cdc2 at the G2/M boundary [33]. Remarkably, the simultaneous manipulation of $cdc25^{+}$ (addition of NLS for nuclear localization) and $wee1^{+}$ (heterozygosity) made diploid cells grow at the same rate and in the same cycle time as haploid cells (Figure 6), supporting again that both genes are key elements to the cell-size scaling with ploidy.

Feedforward network controls CER

Because Wee1 plays a critical role in ploidy-dependent growth control, I asked whether Nim1, known as an inhibitory kinase against Wee1, would control CER dose-dependently. I also examined dose-dependent abilities of Pom1 and Nif1, both acting as negative regulators of Nim1. According to the traditional way of thought, *nim1Δ*/+ heterozygote would activate Wee1 then increase CER whereas *pom1Δ*/+ and *nif1Δ*/+ heterozygotes would activate Nim1 and slow down CER. I observed that both heterozygotes (*Δ*/+) and homozygotes (*Δ*/*Δ*) for each of *pom1Δ* and *nif1Δ* decreased CER (Figures 7(a)), indicating haplo-insufficient positive roles of these genes. They also showed delayed cycle time except the *nif1Δ*/+ strain. Unexpectedly, I observed that *nim1Δ*/+ heterozygote also decreased CER to an equivalent level to the haploid control (Figure 7(a)), indicating a positive role of Nim1. This was confirmed by the observation that double heterozygote *nim1Δ*/+ *pom1Δ*/+, in which Nim1 activity is higher than in the *nim1Δ*/+ heterozygote, grew faster than the *nim1Δ*/+ heterozygote (Figure 7(a)). The *nim1Δ*/+ cells vastly extended cycle time and were finally longer at septation than wild-type cells. However, *nim1Δ*/*nim1Δ* homozygote grew faster than wild-type diploid (Figure 7(a)), indicating a

negative role of Nim1. The *nim1Δ*/*nim1Δ* homozygote also extended cycle time. Together, these results revealed a feedforward network comprised of Nim1, Pom1, and Nif1 acting both as a dose-dependent positive or negative regulator for CER and as a cycle-time keeper.

Nim1 controls nuclear localization of GFP-Wee1 dose-dependently

I asked whether Nim1 would control nuclear localization of GFP-Wee1. I supposed that *nim1Δ*/+ and *nim1Δ*/*nim1Δ* would decrease nuclear GFP-Wee1 as observed in the *cdc25Δ*/+ heterozygote (Figure 4(b)) with the expectation that low Cdc2 activity caused by *nim1Δ*/+ and *nim1Δ*/*nim1Δ* removes GFP-Wee1 from the nuclei. As expected, I observed reduced nuclear localization of GFP-Wee1 in the *nim1Δ*/+ heterozygote (Figure 8(a)(b)). However, I observed increased content of nuclear GFP-Wee1 in the *nim1Δ*/*nim1Δ* homozygote (Figure 8(b)). Together, these results indicate that Nim1 controls nuclear localization of GFP-Wee1 in opposite manners dose-dependently.

To further investigate the activity of Nim1, I examined the effect of increased Nim1 dosage (4x*nim1*$^{+}$) and activity (*pom1Δ*/+ and *pom1Δ*/*pom1Δ*). In all conditions, I observed severe reduction of nuclear localization of GFP-Wee1 at 36.5℃ but no apparent effect at 28℃ (Figure 8(a)(b)). In trial experiments with the *GFP-wee1* background, I observed significant effects of *pom1Δ*/+ as well as *act1Δ*/+ on CER at 36.5℃ but not 28℃ (Supplemental Figure 5). They also showed no effect on CER even at 36.5℃ in the cells harboring *GFP-NESx2-wee1* that expresses Wee1 out of the nucleus (Supplemental Figure 5). These results suggest that the reduction in nuclear localization of GFP-Wee1 at 36.5℃ by the increased Nim1 activity is responsible for the reduced CER. The different effects of the temperatures on the nuclear localization of GFP-Wee1 may occur by lower sensitivity of GFP-Wee1 to Nim1 at 28℃ than at 36.5℃, which coincides with both observations that diploid cells bearing *GFP-wee1* become shorter in length at septation after the temperature shift from 28℃ to 36.5℃ (approximately 10% reduction for 4h) and that nuclear content of GFP-Wee1 is concordantly lower at 36.5℃ than at 28℃ (Figures 4(c), 8(b)). Collectively, these results suggest that Nim1 controls nuclear localization of GFP-Wee1 through two separate pathways, one for nuclear accumulation and another for exclusion from the nuclei.

Next, I examined the effect of the increased dosage of *pom1*+ (4x*pom1*$^{+}$), resulting in reduced nuclear GFP-Wee1 content at 36.5℃ (Figure 8(a)) possibly through partial inhibition of Nim1 as observed in the *nim1Δ*/+ heterozygote. As expected, in the *nim1Δ*/*nim1Δ* background, the *pom1Δ*/+ did not affect the *nim1Δ*-induced nuclear accumulation of GFP-Wee1 (Figure 8(a)).

I also examined the effect of *nif1Δ* on nuclear localization of GFP-Wee1. I observed relatively uniform cellular distribution of GFP-Wee1 at 36.5°C in cells of both *nif1Δ*/+ heterozygote and *nif1Δ*/*nif1Δ* homozygote, indicating a reduction in nuclear localization (Figure 8(a)). Since Nif1, like Pom1, expectedly accumulates GFP-Wee1 in the nucleus through inhibition of Nim1, I also examined the Nim1-dependent ability of Nif1. Unexpectedly, I observed that the *nif1Δ*/*nif1Δ* was so effective as to reduce the nuclear content of GFP-Wee1 in the *nim1Δ*/*nim1Δ* background (Figure 8(a)), suggesting a Nim1-independent role.

I also asked whether the feedforward network would control nuclear localization of GFP-Wee1 in haploid cells. I observed no clear effect in haploid cells bearing *pom1Δ*, *nim1Δ*, or *nif1Δ* (Figure 8(a)), indicating no or limited role of Pom1, Nim1, and Nif1 in haploid.

Since actin dynamics modulate nuclear content of GFP-Wee1 in response to Cdc2 activity, I asked whether the control of nuclear GFP-Wee1 content by the feedforward network would be associated with actin dynamics. To explore this, I examined the effects of *act1-ts* and 3x*act1*$^{+}$ on the reduced nuclear content of GFP-Wee1 in cells harboring each of *pom1Δ*/+, *nim1Δ*/+, *nif1Δ*/+, *nif1Δ*/*nif1Δ*, 4x*pom1*$^{+}$, and 4x*nim1*$^{+}$, and also the effect of *adf1-1* on the increased nuclear content of GFP-Wee1 in the *nim1Δ*/*nim1Δ* cells. I observed clear suppression by *act1-ts*, 3x*act1*$^{+}$, and *adf1-1* (Figures 8(a)). These results indicate that actin dynamics control nuclear content of GFP-Wee1 in concert with the feedforward network.

Feedforward network controls CER both in Wee1-dependent and -independent pathways

Since the feedforward pathway controls CER in association with alteration of nuclear GFP-Wee1 content, I asked whether modulation of Wee1 dosage would affect CER of *nim1Δ*/+ or *pom1Δ*/+ cells. For this purpose, I constructed two types of strains, each harboring *wee1Δ*/+ for half dosage of *wee1*$^{+}$ or 3x*act1*$^{+}$ for increased content of nuclear Wee1. I observed that neither *nim1Δ*/+ nor *pom1Δ*/+ further decreased CER in *wee1Δ*/+ cells (Figure 7(a)), indicating that *wee1Δ*/+ is epistatic to *nim1Δ*/+ and *pom1Δ*/+. Furthermore, the 3x*act1*$^{+}$-induced preservation of nuclear Wee1 also cancelled the defect by *nim1Δ*/+ and *pom1Δ*/+ (Figure 7(a)). These results are consistent with a proposal that Nim1 and Pom1 play a positive role for CER while maintaining nuclear content of Wee1. As expected, *nim1Δ*/*nim1Δ* elevated CER in 3x*act1*$^{+}$ cells significantly (Figure 7(a)), which may occur through both nuclear accumulation of Wee1 and activation of Wee1 kinase activity by relief from the Nim1 inhibitory kinase.

To investigate whether Pom1 and Nif1 control CER through inhibition of Nim1, I examined genetic hierarchy between *nim1Δ* and either *pom1Δ* or *nif1Δ*. The *pom1Δ*/+ did not affect CER of the *nim1Δ*/*nim1Δ* homozygote as expected, while the *pom1Δ*/*pom1Δ* clearly decreased CER in the *nim1Δ*/*nim1Δ* homozygote (Figure 7(a)). The latter result may occur by monopolar extension specific to *pom1Δ*/*pom1Δ* [34]. Next, I observed that the *nif1Δ*/*nif1Δ* decreased CER in the *nim1Δ*/*nim1Δ* homozygote (Figure 7(a)), suggesting a *nim1*$^{+}$-independent positive role of Nif1. This is consistent with the observation that Nif1 is required for the increased accumulation of nuclear GFP-Wee1 in the *nim1Δ*/*nim1Δ* homozygote (Figure 8(a)).

To confirm the genetic cascade in which Wee1 functions at the most upstream position, I constructed strains harboring *wee1Δ*/*wee1Δ* in combination with *nif1Δ*/*nif1Δ* and/or *nim1Δ*/*nim1Δ*. Surprisingly, I observed that *wee1Δ*/*wee1Δ* homozygotes each bearing *nif1Δ*/*nif1Δ*, *nim1Δ*/*nim1Δ*, or *nif1Δ*/*nif1Δ nim1Δ*/*nim1Δ* grew more slowly and were smaller in cell length at division than the *wee1Δ*/*wee1Δ* homozygote (Figure 7(b)), revealing a *wee1*$^{+}$-independent positive role of Nim1 and Nif1. Furthermore, I gave a clear evidence for the positive role of Nim1 in the absence of both *cdc25*$^{+}$ and *wee1*$^{+}$. The *nim1Δ*/*nim1Δ* cells bearing both *cdc25-22/cdc25-22* and *wee1*Δ/*wee1Δ* grew more slowly with shorter cell length at septation than the control cells harboring *cdc25-22/cdc25-22* and *wee1*Δ/*wee1Δ* (Figure 7(c)). Collectively, these results revealed that Nim1 increases CER independently of both Wee1 and Cdc25 possibly playing an inhibitory role against Cdc2. In the present study, Nif1 may control CER in a more complicated manner such that it increases CER through inhibition of Nim1 in the authentic pathway, retention of nuclear Wee1 antagonistically against Nim1, and a Nim1- and Wee1-independent pathway.

Genetic hierarchy between Cdc25 and Nim1

Curiously, Cdc25 and Nim1 regulate CER in both positive and negative manners dose-dependently. To clarify how they control CER cooperatively, I examined genetic hierarchy between Cdc25 and Nim1. For this purpose, I first constructed double heterozygotes harboring *cdc25Δ*/+ and *nim1Δ*/+, and examined growth kinetics and CER. I observed that *cdc25Δ*/+ did not decrease CER in the *nim1Δ*/+ heterozygote, while *nim1Δ*/+ decreased CER in the *cdc25Δ*/+ heterozygote (Figure 9). These results indicate that Nim1 acts downstream of Cdc25 and suggest that Cdc25 serves as a positive regulator in the cascade where Nim1 increases CER. However, the *cdc25Δ*/+ *nim1Δ*/+ double heterozygote further prolonged cycle time compared with the single heterozygotes,

indicating that Cdc25 and Nim1 function to end cell cycle additively or in different pathways.

Next, I asked how Cdc25 regulates CER under the condition where cells express more active Nim1. To explore this, I combined *cdc25Δ*/+ with *pom1Δ*/+ that activates Nim1 and examined the effect of their combination on CER. I observed that *cdc25Δ*/+ increased CER of the *pom1Δ*/+ heterozygote, while *pom1Δ*/+ did not decrease CER of the *cdc25Δ*/+ heterozygote (Figure 9). Since single heterozygosity of *cdc25Δ*/+ and *pom1Δ*/+ decreases CER, these results revealed interdependency between $pom1^{+}$ and $cdc25^{+}$, both acting as positive regulators for CER by accumulating Wee1 in the nuclei. More interestingly, cellular activity (or content) of Nim1 may control action mode of Cdc25: when cells express more active Nim1, Cdc25 serves as a negative regulator.

Actin monomers control CER both in positive and negative manners

The present study suggests that Cdc25 and Nim1 control CER positively through nuclear localization of Wee1 possibly with the aid of actin monomer. I wondered how actin monomers and polymers (or actin cables) work for cell extension at the same time since actin cables and exocytic machineries play parallel roles for polarized growth in fission yeast [15,17]. To clarify this, I first examined the effects of *act1-ts*. Cells pre-grown exponentially at 28℃ were shifted to 36.5℃, and inspected for cell growth. I observed three growth patterns regardless of ploidy (Figure 10(a)): smaller cells at the temperature shift did not grow for about 2 h and thereafter initiated extension (late induction) or a minor fraction of the cells did not grow at all during the experiment (no growth), while longer cells grew immediately (early induction) at moderate CER (Supplemental Figure 6(b)). These results are consistent with the previous report that actin cables are not essential for polarized growth [15] and suggest a specific role of actin filament in the initiation of growth during early G2 phase, or alternatively, that actin monomers inhibit the growth initiation.

I also examined the effect of *act1-ts* in cells with higher or lower Cdc2 activity (induced by *wee1-50* or *cdc25-22*, respectively), because the modulation of Cdc2 activity is effective for gathering early or late G2 cells and for change in actin dynamics: higher or lower Cdc2 activity is expected to strengthen or weaken the effect of *act1-ts*, respectively. As expected, *wee1-50*/*wee1-50* greatly increased population with no growth in *act1-ts*/*act1-ts* diploid (Figure 10(a)), and conversely, *cdc25-22*/*cdc25-22* attenuated the defective growth in *act1-ts*/*act1-ts* or *act1-ts*/*act1-ts wee1-50*/*wee1-50* diploid (Supplemental Figure 6(a)). Haploid *act1-ts* cells responded weakly to the modulation of Cdc2 activity (Supplemental Figure 6(a)). In these experiments, cells with early induction

grew at moderate CER irrespective of ploidy (Supplemental Figure 6(b)). These results further underline a critical role of actin dynamics in the initiation of growth during early G2 phase.

To examine whether Nim1 is involved in the regulation of growth initiation, I used the diploid strain harboring triple mutation (*act1-ts*/*act1-ts*, *cdc25-22*/*cdc25-22*, and *wee1-50*/*wee1-50*) as a control. Half of the population arrested growth after the shift to 36.5℃ (Figure 10(b)). However, *pom1Δ*/+ completely abolished the negative effect of *act1-ts*/*act1-ts*, which was suppressed by further addition of *nim1Δ*/*nim1Δ* (Figure 10(b)). These results suggest that reactivation of Nim1 (caused by *pom1Δ*/+) cancelled the negative effect of *act1-ts*/*act1-ts* on Nim1. Collectively, I propose that actin dynamics affects Nim1 activity directly or indirectly through Pom1 independently of Cdc25 and Wee1. Considering the hypothetical pathway in which Nim1 inhibits Cdc2 (Figure 7(b)(c)), these results suggest that actin dynamics constitute a positive feedback loop, in which Cdc2 stimulates actin monomer formation, resulting in inhibition of Nim1 and feedback activation of Cdc2.

Next, I asked whether the positive feedback loop would account for the increased CER caused by *act1Δ*/+ in *wee1Δ*/+ cells (Figure 3(b)), because the half dosage of $act1^{+}$ is expected to decrease actin monomers, resulting in activation of Nim1, inhibition of Cdc2, and elevation of CER, and additionally because *act1Δ*/+ showed no effect on nuclear content of Cdc25-GFP in *wee1Δ*/+ cells (Figure 5(a)). For this purpose, I examined the effect of *act1Δ*/+ in double heterozygote harboring *wee1Δ*/+ and *nim1Δ*/+ in the hope that the half $nim1^{+}$ dosage would reduce active Nim1. As expected, I observed that *act1Δ*/+ did not elevate but decreased CER of the *wee1Δ*/+ *nim1Δ*/+ heterozygote (Figure 10(c)). The decrease in CER would be caused by reduced activity of the positive pathway in which actin monomers stimulate CER through nuclear localization of Wee1. Together, these results confirm the negative role for CER of the positive feedback loop. I also found that *act1Δ*/+ shortened cycle time in *wee1Δ*/+ cells (Figure 10(c)) as well as in wild-type cells (Figure 3(a)). However, *act1Δ*/+ rather lengthened cycle time of the *wee1Δ*/+ *nim1Δ*/+ heterozygote (Figure 10(c)). These results suggest that actin controls cycle time through Nim1 in the positive feedback pathway.

To verify the positive role of actin monomers, I used the *GFP-NESx2-wee1* background because different kinds of treatment that disrupt normal actin dynamics such as an increased dosage of $act1^{+}$, *act1-ts*, and *adf1-1* did not apparently affect the nuclear exclusion of GFP-NESx2-Wee1 (data not shown). As controls, I examined the effects of *act1-ts*, *adf1-1*, and their combination *act1-ts adf1-1* on CER of diploid cells harboring *GFP-wee1*/*GFP-wee1*. For this purpose, cells grown exponentially at 28℃ were shifted

to 36.5°C and further incubated before cell lysis, during which CER of individual cells was estimated and plotted against initial cell length at the temperature shift. I observed that the cells harboring *act1-ts*/*act1-ts GFP-wee1*/*GFP-wee1* initiated growth immediately without showing late induction found in the *act1-ts*/*act1-ts* cells of normal *wee1*$^{+}$ background (Figure 10(a)) and extended cell length at moderately decreased CER compared with the control bearing *GFP-wee1*/*GFP-wee1* (Figure 10(d)). The absence of the initial growth inhibition may occur because *act1-ts*-induced monomers do not effectively increase Cdc2 activity in the *GFP-wee1*/*GFP-wee1* cells that are longer in cell length (28.9 μm±3.6 for 2n *GFP-wee1*/*GFP-wee1* cells *vs* 22.7 μm±2.2 for 2n wild-type at 28°C in EMM2) and considered to have lower Cdc2 activity than normal *wee1*$^{+}$ diploid. The moderate decrease in CER would occur if increased actin monomers activated the negative route more actively than they did the positive pathway. On the other hand, the *adf1-1*/*adf1-1* cells showed a considerable decrease in CER (Figure 10(d)), which was expected if supposed that substantial decrease in actin monomers by the *adf1-1* mutation would abolish positive route and simultaneously release the suppression from the negative route. If the above speculation would be correct, cells harboring both *adf1-1*/*adf1-1* and *act1-ts*/*act1-ts* would increase monomer forms of actin and recover CER at a similar level to *act1-ts*/*act1-ts* cells. As expected, the double heterozygote showed elevated CER compared with the *adf1-1*/*adf1-1* cells (Figure 10(d)). Next, I made similar experiments using the *GFP-NESx2-wee1* background in the expectation that *act1-ts*-induced increase in actin monomers could not activate positive route but activate negative route normally, then would greatly decrease CER. As expected, I observed that CER was heavily decreased by *act1-ts*/*act1-ts* in diploid cells bearing *GFP-NESx2-wee1*/*GFP-NESx2-wee1* (Figure 10(d)). However, *adf1-1*/*adf1-1* reduced CER of *GFP-NESx2-wee1*/*GFP-NESx2-wee1* cells at the same level as did in the *GFP-wee1*/*GFP-wee1* cells (Figure 10(d)), consistent with the notion that only Nim1 freed from the actin monomer-associated repression activates CER in both cells. Remarkably, *act1-ts*/*act1-ts* did not suppress *adf1-1*/*adf1-1* in diploids bearing *GFP-NESx2-wee1*/*GFP-NESx2-wee1* (Figure 10(d)), confirming a significant positive role of actin monomers in association with nuclear localization of Wee1. Collectively, I propose that actin monomer acts positively on CER through nuclear localization of Wee1 and negatively through inhibition of Nim1 in the positive feedback pathway.

Doubling cell division genes in haploid reproduces diploid growth

Since I identified key genes to ploidy-dependent control of growth rate by deleting one copy of them from diploid, I next explored whether these genes could replicate this

control in haploid by constructing haploid cells bearing two copies of each genes or their combinations. I observed that two copies of *wee1*$^+$ (*GFP-wee1* and *wee1*$^+$) elevated CER effectively as compared with wild-type haploid or a reference haploid bearing *GFP-wee1* (1n *GFP-wee1 wee1Δ*) (Figure 11(a)). However, two copies of *pom1*$^+$ (2x*pom1*$^+$) or *act1*$^+$ (2x*act1*$^+$) did not affect or slightly decreased CER, respectively. As expected, two copies of *cdc25*$^+$ (2x*cdc25*$^+$) and *cdc13*$^+$ (2x*cdc13*$^+$) decreased CER (Figure 11(a)).

Next, I investigated the effect of quintuple combination of two copies of genes (*GFP-wee1* plus *wee1*$^+$, 2x*act1*$^+$, 2x*pom1*$^+$, 2x*cdc25*$^+$, and 2x*cdc13*$^+$). I observed that haploid cells with the quintuple combination showed an equivalent CER to the control diploid (2n *GFP-wee1*/*lys1 wee1Δ*/+), albeit earlier slowdown of CER and consequent shorter cell length at septation (Figure 11(b)). Replacement of *GFP-wee1* with *GFP-NESx2-wee1* and quadruple combinations without each of 2x*act1*$^+$, 2x*pom1*$^+$, 2x*cdc25*$^+$, and 2x*cdc13*$^+$ decreased CER (Figure 11(b)), confirming the dose-dependent positive roles of these genes.

Next, I asked whether two copies of *nim1*$^+$ (2x*nim1*$^+$) could act positively for CER in haploid. For this purpose, I constructed haploids bearing all combinations of 2x*nim1*$^+$, *GFP-wee1* (or *GFP-NESx2-wee1*) plus *wee1*$^+$, 2x*act1*$^+$, 2x*cdc25*$^+$, and 2x*cdc13*$^+$, and examined growth kinetics and CER. I observed that 2x*nim1*$^+$ exclusively increased CER in haploid cells bearing *GFP-wee1* plus *wee1*$^+$, 2x*act1*$^+$, 2x*cdc25*$^+$, and 2x*cdc13*$^+$ at a time and decreased CER in haploid cells with all other combinations (not shown) as shown partly: replacement of *GFP-wee1* with *GFP-NESx2-wee1*, or subtraction of each of 1x*act1*$^+$, 1x*cdc25*$^+$, and 1x*cdc13*$^+$ (Figure 11(c)). The positive effect of 2x*nim1*$^+$ was lost by addition of 2x*pom1*$^+$ (Figure 11(c)), indicating a specific activity of Nim1. Collectively, these results indicate that the dose-dependent positive role of Nim1 works in haploid coordinately with Wee1, actin, Cdc25 and Cdc13. I also observed that 2x*nim1*$^+$ shortened cycle time of the haploid cells bearing two copies of *wee1*$^+$ (*GFP-wee1* plus *wee1*$^+$), 2x*act1*$^+$, 2x*cdc25*$^+$, and 2x*cdc13*$^+$ (Figure 11(c)) but did not of other haploid cells that lacked one of the set (not shown). The shortened cycle time was also recovered by further addition of 2x*pom1*$^+$ (Figure 11(c)). The 2x*nim1*$^+$-induced shortening of cycle time reminds of the prolonged cycle time caused by *nim1Δ*/+ (Figure 7(a)), indicating that Nim1 also works in haploid for control of cycle time coordinately with Wee1, actin, Cdc25, and Cdc13.

Discussion

A model for genetic control of cell-size scaling with ploidy

This study uncovers a genetic mechanism contributing to cell-size scaling with ploidy, and establishes unambiguously that limited numbers of specific genes but not total mass of DNA determine cell size. I propose that systems level control of Cdc2 activity is crucial for cell size determination and that copy number of cell division genes controlling Cdc2 activity is origin of ploidy information (Figure 12(a)). In this model, Cdc2 activity level determines CER during the G2 growth phase: higher or lower Cdc2 activity inhibits or accelerates CER, respectively. Scaling device consists of five pathways, three negative and one positive feedback loops and a feedforward network. In the feedback circuits, Cdc2 controls actin dynamics such that higher Cdc2 activity produces more numbers of actin monomers. They are related to nuclear accumulation of Wee1 and cause lower Nim1 activity in the cytoplasm (or interphase cortical nodes) [35]. The resultant active Wee1 inhibits nuclear Cdc2 activity, which stimulates CER. Conversely, lower Cdc2 activity stimulates actin polymer formation, which is associated with nuclear localization of Cdc25 and subsequent activation of nuclear Cdc2 activity. In the positive feedback loop, actin monomers are involved in activation of cytoplasmic Cdc2 independently of Wee1 through association with the weakened Nim1 activity. Feedforward network consisting of Nim1, Pom1, and Nif1 controls Wee1 activity through the authentic way [6,36,37] while playing an inhibitory role against Cdc2 independently of Wee1. Recently, Cao et al. reported that a synthetic gene circuit generates robust scaling of ring formation with colony size in bacteria, which is mediated by integral feedback and incoherent feedforward control [38]. Thus, this type of regulatory network may be underscored as a common mechanism for biological scaling.

A model for how Nim1 controls nuclear content of Wee1

I propose that the nuclear content of Wee1 observed in the *pom1Δ*/+, +/+ (wild-type), *nim1Δ*/+, and *nim1Δ*/*nim1Δ* cells fluctuated up and down (blue line) by summation of inward (IN) and outward (OUT) amount of Wee1 according to the change in Nim1 activity (Figure 12 (b)). Nim1 controls Cdc2 activity in opposite manners through two independent pathways. It activates Cdc2 by inhibiting Wee1 kinase activity while causes inhibition of Cdc2 separately in the cytoplasm. I propose that the bidirectional activity of Nim1 causes the dose-dependent effects of Nim1 on nuclear content of Wee1 through the control of cytoplasmic Cdc2 activity. In the former pathway (termed import pathway), increasing Nim1 activity leads to nuclear accumulation of Wee1 by inhibition of Wee1

and consequent activation of Cdc2 in the cytoplasm while decreasing Nim1 activity leads to exclusion of Wee1 from the nuclei by activation of Wee1 and resultant inhibition of Cdc2 in the cytoplasm (black line). Conversely, in the latter pathway (termed export), increasing Nim1 activity leads to exclusion of Wee1 from the nuclei by inhibiting cytoplasmic Cdc2 activity while decreasing Nim1 activity leads to nuclear accumulation of Wee1 by activating cytoplasmic Cdc2 activity (light blue line).

Mirror-image relation between CER and nuclear Cdc2 activity

Regulators of Cdc2 activity are present in the cytoplasm and the nucleus while play distinct roles according to the cellular localization (Figure 12(C)). I observed that Cdc25-GFP and GFP-Wee1 increased in nuclear accumulation as diploid cells progressed in G2 except the constant nuclear content of GFP-Wee1 during late G2 (Supplemental Figure 2). Cytoplasmic Nim1 activity is considered to be increased as cells extend their size longitudinally through the relief from Pom1 that localizes at the cell tip [35,39]. Actin undergoes a dynamic change in structure between polymer and monomer in the cytoplasm. As cells progress in G2, polymer forms increasingly while monomer decreases consequently. These regulators control Cdc2 activity and are conversely under the domination of Cdc2 in accordance with the genetically determined pathway (Figure 12(a)). CER increases gradually until middle G2 and thereafter decreases relatively quickly. I propose that CER is finally determined by nuclear Cdc2 activity that is regulated in inverse relation to CER (Figure 12(C)). During early to middle G2, nuclear Cdc2 activity becomes decreased progressively in response to increasing nuclear content of Wee1. Cdc25, Nim1, and actin are responsible for the nuclear accumulation of Wee1, because half dosage of them in diploid cells causes the decrease in nuclear Wee1 content. They also play key roles in increasing nuclear Cdc2 activity during late G2, which may result in a decline in CER and the successful termination of cell extension.

Nucleo-cytoplasmic change in Cdc2 activity

I propose that actin dynamics is central to the regulation of nuclear Wee1 content and Cdc2 activity in diploid cells. Although Cdc2 controls nuclear accumulation of Wee1 in both haploid and diploid cells, actin dynamics is epistatic to Cdc2 in diploid cells while it is not related to the nuclear localization of Wee1 in haploid cells. At early G2, actin monomer stimulates nuclear accumulation of Wee1, which leads to a decrease in the nuclear Cdc2 activity and a subsequent increase in CER (Figure 12(d)). As cells approach to middle G2, increasing Nim1 activity inhibits cytoplasmic Wee1, which activates cytoplasmic Cdc2 activity together with Cdc25. The resulting higher Cdc2 activity in the

cytoplasm may further increase nuclear Wee1 content, which leads to an additional decline in nuclear Cdc2 activity and a simultaneous increase in CER. As the nuclear Cdc2 activity becomes lower, actin begins to form polymer. As cells grow longer, Nim1 activity becomes increasing with a release from the inhibition by both Pom1 and actin monomer. The resulting higher Nim1 activity may cause inhibition of cytoplasmic Cdc2 activity in the Wee1-independent pathway, which makes cells enter into late G2. The cytoplasmic lower Cdc2 activity along with fewer content of actin monomers stimulates exclusion of Wee1 from the nuclei, which may cause activation of nuclear Cdc2 together with incoming Cdc25 into the nuclei which is associated with growing actin polymers. The resulting higher Cdc2 activity in the nucleus begins to decrease CER and finally arrests cell extension.

Here I identified a genetic architecture for control of cell-size scaling with ploidy, however, many issues including molecular details remain unsolved in the present model. It is unknown whether cells form a gradient of Cdc2 activity ranging between the nucleus and the cytoplasm. However, the hypothetical control of Cdc2 activity at different cellular compartments is consistent with the genetic conclusion that Cdc2 activity is required both for the nuclear accumulation of Wee1 and for the consequent low Cdc2 activity that increases CER. I also claim that higher Nim1 activity should be the trigger for entering into late G2 or the CER-decreasing period. For this purpose, Nim1 is hypothesized to eventually inhibit Cdc2 activity in the cytoplasm independently of Wee1. This can be inferred from the genetic data that Nim1 not only increases CER in the absence of Wee1 (Figures 7(b)(c)) but also removes nuclear Wee1 dependently upon actin dynamics which is under the control of Cdc2 (Figures 4(a), 8(a)). Finally, future works should shed light on how actin dynamics is related with nuclear accumulation of Wee1 and Cdc25. It is of great interest whether actin dynamics plays a pivotal role in the yeast nuclear transport system as in mammalian cells [40]. Regardless of the exact mechanism, my findings have important implications for understanding a longstanding and universal issue ‘DNA content-cell size rule’ in other eukaryotes including plants and animals, in which polyploidy may control tissue-specific cell size and function [5,41]. Finally, my results may advance agricultural application to breeding of crops and gardening plants and lay the groundwork for therapy of diseases in which polyploid cells are involved.

Acknowledgements

I thank P. Russell, P. Nurse, J. Bähler, J. R. Pringle, J. Ishiguro, P. G. Young, H. Masuda, K. Kitamura, K. Kume, D. Hirata and the National Bio-Resource Project (NBRP) Japan for reagents and T. Toda, M. Mizunuma and K. Kume for discussions.

Disclosure statement

The author declares that he has no conflict of interest.

References

[1] Kondorosi E, Roudier F, Gendreau E. Plant cell-size control: growing by ploidy? Curr Opin Plant Biol. 2000;3:488-492.

[2] Cavalier-Smith T. Economy, speed and size matter: evolutionary forces driving nuclear genome miniaturization and expansion. Ann Botany. 2005;95:147-175.

[3] Gregory TR. The C-value enigma in plants and animals: a review of parallels and an appeal for partnership. Ann Botany. 2005;95:133-146.

[4] Hyun OL, Jean MD, Robert JD. Endoreplication: polyploidy with purpose. Genes Dev. 2009;23:2461-2477.

[5] Orr-Weaver TL. When bigger is better: the role of polyploidy in organogenesis. Trends Genet. 2015;31:307-315.

[6] Wood E, Nurse P. Sizing up to divide: mitotic cell-size control in fission yeast. Ann Rev Cell Dev Biol. 2015;31:11-29.

[7] Booher R, Beach D. Involvement of *cdc13*$^{+}$ in mitotic control in *Schizosaccharomyces pombe*: possible interaction of the gene product with microtubules. EMBO J. 1988;7:2321-2327.

[8] Russell P, Nurse P. Negative regulation of mitosis by *wee1*$^{+}$, a gene encoding a protein kinase homolog. Cell. 1987;49:559-567.

[9] Russell P, Nurse P. *cdc25*$^{+}$ functions as an inducer in the mitotic control of fission yeast. Cell. 1986;45:145-153.

[10] Russell P, Nurse P. The mitotic Inducer *nim1*$^{+}$ functions in a regulatory network of protein kinase homologs controlling the initiation of mitosis. Cell. 1987;49:569-576.

[11] Feilotter H, Nurse P, Young PG. Genetic and molecular analysis of *cdr1*/*nim1* in *Schizosaccharomyces pombe*. Genetics. 1991;127:309-318.

[12] Bähler J, Pringle JR. Pom1p, a fission yeast protein kinase that provides positional information for both polarized growth and cytokinesis. Genes Dev. 1998;12:1356-1370.

[13] Wu L, Russell P. Nif1, a novel mitotic inhibitor in *Schizosaccharomyces pombe*. EMBO J. 1997;16:1342-1350.

[14] Ishiguro J, Kobayashi W. An actin point-mutation neighboring the 'hydrophobic plug' causes defects in the maintenance of cell polarity and septum organization in the fission yeast *Schizosaccharomyces pombe*. FEBS Lett. 1996;392:237-241.

[15] Bendezú FO, Martin SG. Actin cables and the exocyst form two independent morphogenesis pathways in the fission yeast. Mol Biol Cell. 2011;22:44-53.

[16] Kovar DR, Sirotkin V, Lord M. Three's company: the fission yeast actin cytoskeleton. Trends Cell Biol. 2011;21:177-187.

[17] Hammer JA3rd, Sellers JR. Walking to work: roles for class V myosins as cargo transporters. Nat Rev Mol Cell Biol. 2012;13:13-26.

[18] Kellogg DR. Wee1-dependent mechanisms required for coordination of cell growth and cell division. J Cell Sci. 2003;116:4883-4890.

[19] Sveiczer A, Novak B, Mitchison JM. The size control of fission yeast revisited. J Cell Sci. 1996;109:2947-2957.

[20] Adams J, Hansche PE. Population studies in microorganism I. evolution of diploidy in *Sacchromyces cerevisiae*. Genetics. 1974;76:327-338.

[21] Sugiyama S. Polyploidy and cellular mechanisms changing leaf size: comparison of diploid and autotetraploid populations in two species of *Lolium*. Ann Botany. 2005;96:931-938.

[22] Zhou Y, Wang M, Jiang M, et al. Autotetraploid cell Line induced by SP600125 from crucian carp and its developmental potentiality. Sci Rep. 2016;6:21814.

[23] Gould KL, Nurse P. Tyrosine phosphorylation of the fission yeast *cdc2*$^{+}$ protein kinase regulates entry into mitosis. Nature. 1989;342:39-45.

[24] Chua G, Lingner C, Frazer C, et al. The *sal3*$^{+}$ gene encodes an importin-β implicated in the nuclear import of Cdc25 in *Schizosaccharomyces pombe*. Genetics. 2002;162:689-703.

[25] Masuda H, Fong CS, Ohtsuki C, et al. Spatiotemporal regulations of Wee1 at the G2/M transition. Mol Biol Cell. 2011;22:555-569.

[26] Rothstein RJ. One-step gene disruption in yeast. Meth Enzymol. 1983;101:202-211.

[27] Sabatinos SA, Forsburg SL. Molecular genetics of *Schizosaccharomyces pombe*. Meth Enzymol. 2010;470:759-795.

[28] Verde F, Mata J, Nurse P. Fission yeast cell morphogenesis: identification of new genes and analysis of their role during the cell cycle. J Cell Biol. 1995;131:1529-1538.

[29] Verde F, Wiley DJ, Nurse P. Fission yeast *orb6*, a ser/thr protein kinase related to mammalian rho kinase and myotonic dystrophy kinase, is required for maintenance of cell polarity and coordinates cell morphogenesis with the cell cycle. Proc Nat Acad Sci USA. 1998;95:7526-7531.

[30] Kamasaki T, Arai R, Osumi M, et al. Directionality of F-actin cables changes during the fission yeast cell cycle. Nat Cell Biol. 2005;7:916-917.

[31] Nakano K, Mabuchi I. Actin-depolymerizing protein Adf1 is required for formation and maintenance of the contractile ring during cytokinesis in fission yeast. Mol Biol Cell. 2006;17:1933-1945.

[32] Rupeš I, Webb BA, Mak A, et al. G2/M arrest caused by actin disruption is a manifestation of the cell size checkpoint in fission yeast. Mol Biol Cell. 2001;12:3892-3903.

[33] Lu LX, Domingo-Sananes MR, Huzarska M, et al. Multisite phosphoregulation of Cdc25 activity refines the mitotic entrance and exit switches. Proc Nat Acad Sci USA. 2012;109:9899-9904.

[34] Bhatia P, Hachet O, Hersch M, et al. Distinct levels in Pom1 gradients limit Cdr2 activity and localization to time and position division. Cell Cycle. 2014;13:538-552.

[35] Moseley JB, Mayeux A, Paoletti A, et al. A spatial gradient coordinates cell size and mitotic entry in fission yeast. Nature. 2009;459:857-860.

[36] Marshall WF, Young KD, Swaffer M, et al. What determines cell size? BMC Biol. 2012;10:101.

[37] Zhu YH, Wu JQ. Cell-size control: complicated. Cell Cycle. 2014;13:693-694.

[38] Cao Y, Ryser MD, Payne S, et al. Collective space-sensing coordinates pattern scaling in engineered bacteria. Cell. 2016;165:620-630.

[39] Martin SG, Berthelot-Grosjean M. Polar gradients of the DYRK-family kinase Pom1 couple cell length with the cell cycle. Nature. 2009;459:852-856.

[40] Vartiainen MK, Guettler S, Larijani B, et al. Nuclear actin regulates dynamic subcellular localization and activity of the SRF cofactor MAL. Science. 2007;316:1749-1752.

[41] Pandit SK, Westendorp B, de Bruin A. Physiological significance of polyploidization in mammalian cells. Trends Cell Biol. 2013;23:556-566.

Figure 1. Diploid cells grow faster than haploid cells.
(a) Time-lapse images of wild-type haploid (1n) and diploid (2n) cells at 28℃. Photographs were taken every 30 min. Arrowheads indicate the same growing cells. Bar, 10 μm. (b) Growth kinetics (*top*) and CER (*bottom*), starting from one division to the next.

Figure 2. Cell division genes control cell growth.
CER of the wild-type and temperature-sensitive mutants as indicated after the shift to 36.5℃.

Figure 3. Haplo-insufficient roles of cell division genes.
(a) Growth kinetics and (b) maximum CER during incubation at 28℃ of the heterozygotes indicated. The *wee1Δ*/*wee1Δ* strain was used as a reference. Data for wild-type cells are the same as shown in Figure 1. Statistical significance (*p* value) against the strain marked by bar is presented. (c) A hypothetical genetic pathway. Arrow and T-bar indicate activation and repression, respectively.

Figure 4. Cdc2 and actin dynamics control nuclear localization of GFP-Wee1.
(a) Nuclear localization of GFP-Wee1 at 28℃ and after the shift to 36.5℃ for 20 and 30 min in the haploid and diploid cells indicated, respectively. (b, c) Fluorescence images of live cells. Bar, 10 μm.

Figure 5. Cdc2 and actin dynamics control nuclear localization of Cdc25-GFP.
(a) Nuclear localization of Cdc25-GFP or Cdc25-NLS-GFP at 28℃ and after the shift to 36.5℃ for 1 or 2 h. (b, c) Fluorescence images of live cells. Bar, 10 μm.

Figure 6. Positive roles of Cdc25 both in CER and division timing.
Growth kinetics and maximum CER at 28℃ of the cells harboring *cdc25-GFP* or *cdc25-NLS-GFP*.

Figure 7. Feedforward network controls CER.
(a-c) Growth kinetics and maximum CER at 28℃ (a, b) and 36.5℃ (c).

Figure 8. Feedforward network controls nuclear localization of GFP-Wee1.
(a) Nuclear localization of GFP-Wee1 at 28℃ and after the shift to 36.5℃ for 20 and 30 min in the haploid and diploid cells, respectively. (b) Fluorescence images of live cells. Intensity of nuclear GFP-Wee1 is also presented. Bar, 10 μm.

Figure 9. Genetic hierarchy between Cdc25 and Nim1.
Growth kinetics and maximum CER at 28℃.

Figure 10. Actin monomers control CER both in positive and negative manners.
(a) Actin dynamics controls the initiation of growth at early G2. Growth kinetics and maximum CER of individual *act1-ts* cells after the shift to 36.5℃ plotted against initial cell length at the temperature shift. Early and late induction of growth was represented by blue and red marks, respectively. No growth during the incubation was by bright green. (b) Actin dynamics affects cell growth through Pom1-Nim1. (c) Actin controls both CER and cycle time through Nim1. (d) Actin monomer controls CER both positively through nuclear localization of Wee1 and negatively in a separate pathway.

Figure 11. Doubling cell division genes in haploid reproduces diploid growth.
(a-c) Growth kinetics and maximum CER at 36.5℃. (a) Haploids each bearing two copies of *cdc13*$^{+}$, *cdc25*$^{+}$, *pom1*$^{+}$, *act1*$^{+}$, or *wee1*$^{+}$ (*GFP-wee1* and *wee1*$^{+}$) and haploid controls (wild and *GFP-wee1 wee1Δ*). (b) A haploid bearing quintuple combination of the two copies of genes and haploids bearing quadruple combination that lack one of five. Diploid control (2n *GFP-wee1*/*lys1 wee1Δ*/+) is also shown. (c) Positive role of Nim1 in haploid. Series of haploids bearing quadruple or triple combination and those bearing in addition two copies of *nim1*$^{+}$ (2x*nim1*$^{+}$) or 2x*nim1*$^{+}$ plus 2x*pom1*$^{+}$.

Figure 12. A model for how fission yeast cells scale their size with ploidy.
(a) Genetic framework for control of CER in diploid. Arrow and T-bar indicate activation and repression, respectively. (b) Nim1 controls nuclear content of Wee1 through two different pathways. Blue circle, nuclear Wee1 content observed in the strains indicated. Black circle, hypothetical current of Wee1 into (IN) or out (OUT) of the nucleus through the import pathway. Light blue circle, that through the export pathway. (c) Proposed fluctuation of protein content or activity in the nucleus and cytoplasm together with CER during G2 progression in diploid cells. Values are relative in each protein and not comparable among proteins. (d) Nucleo-cytoplasmic change in Cdc2 activity during G2 progression. Arrows indicate flow of Wee1 and Cdc25 into and out of the nucleus. The Wee1 oval with dotted slant lines indicates inhibition by Nim1. Cytoplasmic areas of active Pom1 and Nim1 are colored yellow and brown, respectively. Actin monomers and polymers are presented by oval and its chain, respectively.

Supplemental Figure 1. Fluorescence images of actin.
Cells pre-grown exponentially at 28℃ in EMM2 (or supplemented with requirements) were incubated at 36.5℃ for 4 h before staining with rhodamine-phalloidin as described previously [32]. Bar, 10 μm.

Supplemental Figure 2. Fluorescence images of GFP-Wee1 and Cdc25-GFP.
Cells were cultured exponentially at 28℃ in EMM2. Total contents of GFP-Wee1 and Cdc25-GFP (in arbitrary unit) in the nuclei of individual cells were plotted against cell length. Bar, 10 μm.

Supplemental Figure 3. Effects of *cdc2-3w* on nuclear localization of GFP-Wee1 and GFP-NESx2-Wee1.
Cells were cultured exponentially at 28℃ in EMM2. Nuclear intensity of GFP-Wee1 also shown. Bar, 10 μm.

Supplemental Figure 4. Actin dynamics controls nuclear localization of Cdc25-GFP.
Cells were grown at 28℃, and viewed by fluorescence microscopy for nuclear localization of Cdc25-GFP and Cdc25-NLS-GFP after the treatment with latrunculin A (10 μM) or DMSO for the indicated time. Bar, 10 μm.

Supplemental Figure 5. Effect of the temperature on CER in the cells bearing *GFP-wee1* and *GFP-NESx2-wee1*.
CER was measured at 28℃ and 36.5℃ in the cells bearing *GFP-wee1* and *GFP-NESx2-wee1*. Heterozygosity of *act1Δ* and *pom1Δ* decreased CER only at 36.5℃ in the *GFP-wee1* background.

Supplemental Figure 6. Actin dynamics controls cell growth cooperatively with Cdc2.
(a, b) Cells were cultured at 36.5℃. (a) Proportion of cells showing early or late induction and no growth. (b) Average values of maximum CER in the individual cells showing early induction.

Supplemental Table 1. The *S. pombe* strains used.

Experiment	Strain	Genotype
Figure 1	2802	h^{-} wild
	2829	h$^{+/-}$ *ade6-M210/ade6-M216*
Figure 2	2802	h^{-} wild
	2829	h$^{+/-}$ *ade6-M210/ade6-M216*
	3967	h^{-} *wee1-50*
	4031	h$^{+/-}$ *wee1-50/wee1-50 leu1-32/+ ade6-M210/ade6-M216*
	3823	h^{-} *cdc25-22*
	3691	h$^{+/-}$ *cdc25-22/cdc25-22 ade6-M210/ade6-M216*
	3779	h^{-} *cdc2-L7*
	3800	h$^{+/-}$ *cdc2-L7/cdc2-L7 ade6-M210/ade6-M216*
	4017	h^{-} *cdc13-117*
	4035	h$^{+/-}$ *cdc13-117/cdc13-117 ade6-M210/ade6-M216*
Figure 3	2802	h^{-} wild
	2829	h$^{+/-}$ *ade6-M210/ade6-M216*
	5646	h$^{-/-}$ *cdc25Δ::ura4^{+}/+ leu1-32/+ ura4-D18/ura4-D18 ade6-M210/ade6-M216*
	4684	h$^{+/-}$ *wee1Δ::ura4^{+}/+ leu1-32/+ ura4-D18/ura4-D18 ade6-M210/ade6-M216*
	5649	h$^{-/-}$ *act1Δ::ura4^{+}/+ leu1-32/+ ura4-D18/ura4-D18 ade6-M210/ade6-M216*
	5667	h$^{+/+}$ *cdc25Δ::ura4^{+}/+ wee1Δ::ura4^{+}/+ leu1-32/+ ura4-D18/ura4-D18 ade6-M210/ade6-M216*
	5670	h$^{-/-}$ *act1Δ::ura4^{+}/+ cdc25Δ::ura4^{+}/+ leu1-32/+ ura4-D18/ura4-D18 ade6-M210/ade6-M216*
	5669	h$^{-/-}$ *act1Δ::ura4^{+}/+ wee1Δ::ura4^{+}/+ leu1-32/+ ura4-D18/ura4-D18 ade6-M210/ade6-M216*
	6021	h$^{-/-}$ *cdc25Δ::ura4^{+}/+ wee1Δ::ura4^{+}/+ act1Δ::ura4^{+}/+ leu1-32/+* (or +/+) *ura4-D18/ura4-D18 ade6-M210/ade6-M216*
	4688	h$^{+/-}$ *wee1Δ::ura4^{+}/wee1Δ::ura4^{+} leu1-32/+ ura4-D18/ura4-D18 ade6-M210/ade6-M216*
Figure 4	3174	h^{+} *lys1^{+}::GFP-wee1 wee1Δ::ura4^{+} ura4-D18*
	3234	h^{-} *cdc2-3w lys1^{+}::GFP-wee1 wee1Δ::ura4^{+} ura4-D18*

Figure 4	3707	h^{-} *cdc2-L7 lys1^{+}::GFP-wee1 wee1Δ::ura4^{+} ura4-D18* (or *-294*)
	3891	h^{+} *cdc25-22 lys1^{+}::GFP-wee1 wee1Δ::ura4^{+} ura4-D18 ade6-M210*
	4042	h^{+} *cdc13-117 lys1^{+}::GFP-wee1 wee1Δ::ura4^{+} ura4-D18*
	4181	h^{+} *2xact1^{+}::ura4^{+} lys1^{+}::GFP-wee1 wee1Δ::ura4-3233 ura4-D18*
	5701	h^{+} *cdc13-117 2xact1^{+}::ura4^{+} lys1^{+}::GFP-wee1 wee1Δ::ura4-3233 ura4-D18 ade6-M210*
	1371	h^{-} *act1-ts lys1^{+}::GFP-wee1 wee1Δ::ura4^{+} leu1-32 ura4-D18*
	5685	h^{-} *act1-ts cdc13-117 lys1^{+}::GFP-wee1 wee1Δ::ura4^{+} leu1-32 ura4-D18 ade6-M210*
	4699	h^{-} *adf1-1 lys1^{+}::GFP-wee1 wee1Δ::ura4^{+} ura4-D18*
	5301	h^{-} *adf1-1 cdc2-3w lys1^{+}::GFP-wee1 wee1Δ::ura4^{+} ura4-D18*
	3180	h$^{+/-}$ *lys1^{+}::GFP-wee1/lys1^{+}::GFP-wee1 wee1Δ::ura4^{+}/wee1Δ::ura4^{+} leu1-32/+ ura4-D18/ura4-D18 ade6-M210/ade6-M216*
	3256	h$^{+/-}$ *cdc2-3w/cdc2-3w lys1^{+}::GFP-wee1/lys1^{+}::GFP-wee1 wee1Δ::ura4^{+}/wee1Δ::ura4^{+} ura4-D18/ura4-D18 ade6-M210/ade6-M216*
	3728	h$^{+/-}$ *cdc2-L7/cdc2-L7 lys1^{+}::GFP-wee1/lys1^{+}::GFP-wee1 wee1Δ::ura4^{+}/wee1Δ::ura4^{+} ura4-D18* (or *-294*)*/ura4-D18* (or *-294*) *ade6-M210/ade6-M216*
	3892	h$^{+/-}$ *cdc25-22/cdc25-22 lys1^{+}::GFP-wee1/lys1^{+}::GFP-wee1 wee1Δ::ura4^{+}/wee1Δ::ura4^{+} leu1-32/+ ura4-D18/ura4-D18 ade6-M210/ade6-M216*
	4060	h$^{+/-}$ *cdc13-117/cdc13-117 lys1^{+}::GFP-wee1/lys1^{+}::GFP-wee1 wee1Δ::ura4^{+}/wee1Δ::ura4^{+} ura4-D18/ura4-D18 ade6-M210/ade6-M216*
	3452	h$^{-/-}$ *cdc25Δ::ura4^{+}/+ lys1^{+}::GFP-wee1/lys1^{+}::GFP-wee1 wee1Δ::ura4-3233/wee1Δ::ura4-3233 leu1-32/+ ura4-D18/ura4-D18 ade6-M210/ade6-M216*

Figure 4	3927	h$^{-/-}$ *cdc13Δ::ura4*$^{+}$/+ *lys1*$^{+}$*::GFP-wee1/lys1*$^{+}$*::GFP-wee1 wee1Δ::ura4-3233/wee1Δ::ura4-3233 leu1-32/+ ura4-D18/ura4-D18 ade6-M210/ade6-M216*
	3322	h$^{+/-}$ *act1Δ::ura4*$^{+}$/+ *lys1*$^{+}$*::GFP-wee1/lys1*$^{+}$*::GFP-wee1 wee1Δ::ura4-3233/wee1Δ::ura4-3233 leu1-32/+ ura4-D18/ura4-D18 ade6-M210/ade6-M216*
	4813	h$^{+/-}$ 2x*act1*$^{+}$*::ura4*$^{+}$/+ (3x*act1*$^{+}$) *lys1*$^{+}$*::GFP-wee1/lys1*$^{+}$*::GFP-wee1 wee1Δ::ura4-3233/wee1Δ::ura4-3233 ura4-D18/ura4-D18 ade6-M210/ade6-M216*
	5731	h$^{+/-}$ *cdc13-117/cdc13-117* 2x*act1*$^{+}$*::ura4*$^{+}$/+ (3x*act1*$^{+}$) *lys1*$^{+}$*::GFP-wee1/lys1*$^{+}$*::GFP-wee1 wee1Δ::ura4-3233/wee1Δ::ura4-3233 ura4-D18/ura4-D18 ade6-M210/ade6-M216*
	4951	h$^{+/-}$ *cdc25Δ::ura4*$^{+}$/+ 2x*act1*$^{+}$*::ura4*$^{+}$/+ (3x*act1*$^{+}$) *lys1*$^{+}$*::GFP-wee1/lys1*$^{+}$*::GFP-wee1 wee1Δ::ura4-3233/wee1Δ::ura4-3233 ura4-D18/ura4-D18 ade6-M210/ade6-M216*
	4953	h$^{-/-}$ *cdc13Δ::ura4*$^{+}$/+ 2x*act1*$^{+}$*::ura4*$^{+}$/+ (3x*act1*$^{+}$) *lys1*$^{+}$*::GFP-wee1/lys1*$^{+}$*::GFP-wee1 wee1Δ::ura4-3233/wee1Δ::ura4-3233 ura4-D18/ura4-D18 ade6-M210/ade6-M216*
	3636	h$^{+/-}$ *act1-ts/act1-ts lys1*$^{+}$*::GFP-wee1/lys1*$^{+}$*::GFP-wee1 wee1Δ::ura4*$^{+}$*/wee1Δ::ura4-3233 leu1-32/+ ura4-D18/ura4-D18 ade6-M210/ade6-M216*
	5691	h$^{+/-}$ *act1-ts/act1-ts cdc13-117/cdc13-117 lys1*$^{+}$*::GFP-wee1/lys1*$^{+}$*::GFP-wee1 wee1Δ::ura4*$^{+}$*/wee1Δ::ura4*$^{+}$ *leu1-32/leu1-32 ura4-D18/ura4-D18 ade6-M210/ade6-M216*
	4734	h$^{+/-}$ *adf1-1/adf1-1 lys1*$^{+}$*::GFP-wee1/lys1*$^{+}$*::GFP-wee1 wee1Δ::ura4*$^{+}$*/wee1Δ::ura4*$^{+}$ *ura4-D18/ura4-D18 ade6-M210/ade6-M216*
	4854	h$^{+/-}$ *act1-ts/act1-ts adf1-1/adf1-1 lys1*$^{+}$*::GFP-wee1/lys1*$^{+}$*::GFP-wee1 wee1Δ::ura4*$^{+}$*/wee1Δ::ura4*$^{+}$ *ura4-D18/ura4-D18 ade6-M210/ade6-M216*

Figure 4	5320	h$^{+/-}$ *adf1-1/adf1-1 cdc2-3w/cdc2-3w lys1^{+}::GFP-wee1/lys1^{+}::GFP-wee1 wee1Δ::ura4^{+}/wee1Δ::ura4^{+} ura4-D18/ura4-D18 ade6-M210/ade6-M216*
Figure 5	1461	h^{-} *cdc25Δ::ura4^{+}::cdc25-GFP::leu1^{+} leu1-32 ura4-D18*
	1557	h^{-} *cps8-188* (*act1-ts*) *cdc25Δ::ura4^{+}::cdc25-GFP::leu1^{+} leu1-32 ura4-D18 ade6-M210*
	4708	h^{-} *adf1-1 cdc25Δ::ura4^{+}::cdc25-GFP::leu1^{+} leu1-32 ura4-D18*
	1464	h^{-} *wee1-50 cdc25Δ::ura4^{+}::cdc25-GFP::leu1^{+} leu1-32 ura4-D18*
	1846	h^{-} *cdc13-117 cdc25Δ::ura4^{+}::cdc25-GFP::leu1^{+} leu1-32 ura4-D18 ade6-M210*
	1909	h^{-} *act1-ts cdc13-117 cdc25Δ::ura4^{+}::cdc25-GFP::leu1^{+} leu1-32 ura4-D18 ade6-M210*
	4780	h^{-} *adf1-1 cdc13-117 cdc25Δ::ura4^{+}::cdc25-GFP::leu1^{+} leu1-32 ura4-D18*
	1587	h^{-} *cdc25Δ::ura4^{+}::cdc25-NLS-GFP::leu1^{+} leu1-32 ura4-D18 ade6-M216*
	1870	h^{-} *wee1-50 cdc25Δ::ura4^{+}::cdc25-NLS-GFP::leu1^{+} leu1-32 ura4-D18*
	2792	h^{+} *act1-ts cdc25Δ::ura4^{+}::cdc25-NLS-GFP::leu1^{+} leu1-32 ura4-D18 ade6-M210*
	4796	h^{-} *adf1-1 cdc25Δ::ura4^{+}::cdc25-NLS-GFP::leu1^{+} leu1-32 ura4-D18*
	3614	h$^{-/-}$ *cdc25Δ::ura4^{+}::cdc25-GFP::leu1^{+}/ cdc25Δ::ura4^{+}::cdc25-GFP::leu1^{+} leu1-32/leu1-32 ura4-D18/ura4-D18 ade6-M210/ade6-M216*
	1740	h$^{+/-}$ *act1-ts/act1-ts cdc25Δ::ura4^{+}::cdc25-GFP::leu1^{+}/ cdc25Δ::ura4^{+}::cdc25-GFP::leu1^{+} leu1-32/leu1-32 ura4-D18/ura4-D18 ade6-M210/ade6-M216*
	4736	h$^{+/-}$ *adf1-1/adf1-1 cdc25Δ::ura4^{+}::cdc25-GFP::leu1^{+}/ cdc25Δ::ura4^{+}::cdc25-GFP::leu1^{+} leu1-32/leu1-32 ura4-D18/ura4-D18 ade6-M210/ade6-M216*

Figure 5	1488	h$^{+/-}$ *wee1-50/wee1-50 cdc25Δ::ura4^{+}::cdc25-GFP::leu1^{+}/ cdc25Δ::ura4^{+}::cdc25-GFP::leu1^{+} leu1-32/leu1-32 ura4-D18/ura4-D18 ade6-M210/ade6-M216*
	1861	h$^{+/-}$ *cdc13-117/cdc13-117 cdc25Δ::ura4^{+}::cdc25-GFP::leu1^{+}/ cdc25Δ::ura4^{+}::cdc25-GFP::leu1^{+} leu1-32/leu1-32 ura4-D18/ura4-D18 ade6-M210/ade6-M216*
	1925	h$^{+/-}$ *act1-ts/act1-ts cdc13-117/cdc13-117 cdc25Δ::ura4^{+}::cdc25-GFP::leu1^{+}/ cdc25Δ::ura4^{+}::cdc25-GFP::leu1^{+} leu1-32/leu1-32 ura4-D18/ura4-D18 ade6-M210/ade6-M216*
	4808	h$^{+/-}$ *adf1-1/adf1-1 cdc13-117/cdc13-117 cdc25Δ::ura4^{+}::cdc25-GFP::leu1^{+}/ cdc25Δ::ura4^{+}::cdc25-GFP::leu1^{+} leu1-32/leu1-32 ura4-D18/ura4-D18 ade6-M210/ade6-M216*
	3592	h$^{-/-}$ *wee1Δ::ura4^{+}/+ cdc25Δ::ura4-2012::cdc25-GFP::leu1^{+}/ cdc25Δ::ura4-2012::cdc25-GFP::leu1^{+} leu1-32/leu1-32 ura4-D18/ura4-D18 ade6-M210/ade6-M216*
	2141	h$^{-/-}$ *act1Δ::ura4^{+}/+ cdc25Δ::ura4-2012::cdc25-GFP::leu1^{+}/ cdc25Δ::ura4-2012::cdc25-GFP::leu1^{+} leu1-32/leu1-32 ura4-D18/ura4-D18 ade6-M210/ade6-M216*
	3705	h$^{-/-}$ *act1Δ::ura4^{+}/+ wee1Δ::ura4^{+}/+ cdc25Δ::ura4-2012::cdc25-GFP::leu1^{+}/ cdc25Δ::ura4-2012::cdc25-GFP::leu1^{+} leu1-32/leu1-32 ura4-D18/ura4-D18 ade6-M210/ade6-M216*
	6134	h$^{+/-}$ *cdc25Δ::ura4^{+}::cdc25-NLS-GFP::leu1^{+}/ cdc25Δ::ura4^{+}::cdc25-NLS-GFP::leu1^{+} leu1-32/leu1-32 ura4-D18/ura4-D18 ade6-M210/ade6-M216*
	1886	h$^{+/-}$ *wee1-50/wee1-50 cdc25Δ::ura4^{+}::cdc25-NLS-GFP::leu1^{+}/ cdc25Δ::ura4^{+}::cdc25-NLS-GFP::leu1^{+} leu1-32/leu1-32 ura4-D18/ura4-D18 ade6-M210/ade6-M216*

Figure 5	2797	h$^{+/-}$ *act1-ts/act1-ts cdc25Δ::ura4^{+}::cdc25-NLS-GFP::leu1^{+}/ cdc25Δ::ura4^{+}::cdc25-NLS-GFP::leu1^{+} leu1-32/leu1-32 ura4-D18/ura4-D18 ade6-M210/ade6-M216*
	4811	h$^{+/-}$ *adf1-1/adf1-1 cdc25Δ::ura4^{+}::cdc25-NLS-GFP::leu1^{+}/ cdc25Δ::ura4^{+}::cdc25-NLS-GFP::leu1^{+} leu1-32/leu1-32 ura4-D18/ura4-D18 ade6-M210/ade6-M216*
	6139	h$^{+/-}$ *wee1Δ::ura4^{+}/+ cdc25Δ::ura4^{+}::cdc25-NLS-GFP::leu1^{+}/ cdc25Δ::ura4^{+}::cdc25-NLS-GFP::leu1^{+} leu1-32/leu1-32 ura4-D18/ura4-D18 ade6-M210/ade6-M216*
Figure 6	1461	h^{-} *cdc25Δ::ura4^{+}::cdc25-GFP::leu1^{+} leu1-32 ura4-D18*
	3614	h$^{-/-}$ *cdc25Δ::ura4^{+}::cdc25-GFP::leu1^{+}/ cdc25Δ::ura4^{+}::cdc25-GFP::leu1^{+} leu1-32/leu1-32 ura4-D18/ura4-D18 ade6-M210/ade6-M216*
	3592	h$^{-/-}$ *wee1Δ::ura4^{+}/+ cdc25Δ::ura4-2012::cdc25-GFP::leu1^{+}/ cdc25Δ::ura4-2012::cdc25-GFP::leu1^{+} leu1-32/leu1-32 ura4-D18/ura4-D18 ade6-M210/ade6-M216*
	6112	h^{-} *cdc25Δ::ura4^{+}::cdc25-NLS-GFP::leu1^{+} leu1-32 ura4-D18*
	6134	h$^{+/-}$ *cdc25Δ::ura4^{+}::cdc25-NLS-GFP::leu1^{+}/ cdc25Δ::ura4^{+}::cdc25-NLS-GFP::leu1^{+} leu1-32/leu1-32 ura4-D18/ura4-D18 ade6-M210/ade6-M216*
	6139	h$^{+/-}$ *wee1Δ::ura4^{+}/+ cdc25Δ::ura4^{+}::cdc25-NLS-GFP::leu1^{+}/ cdc25Δ::ura4^{+}::cdc25-NLS-GFP::leu1^{+} leu1-32/leu1-32 ura4-D18/ura4-D18 ade6-M210/ade6-M216*
Figure 7	2802	h^{-} wild
	2829	h$^{+/-}$ *ade6-M210/ade6-M216*
	6136	h$^{+/-}$ *nim1Δ::LEU2/+ leu1-32/leu1-32 ade6-M210/ade6-M216*
	4445	h$^{+/-}$ *nim1Δ::LEU2/ nim1Δ::LEU2 leu1-32/leu1-32 ura4-D18/+ ade6-M210/ade6-M216*

Figure 7	6057	h$^{-/-}$ *pom1Δ::ura4*$^{+}$/+ *leu1-32*/+ *ura4-D18/ura4-D18 ade6-M210/ade6-M216*
	4975	h$^{+/-}$ *pom1Δ::ura4*$^{+}$/*pom1Δ::ura4*$^{+}$ *ura4-D18/ura4-D18 ade6-M210/ade6-M216*
	6114	h$^{+/-}$ *nif1Δ::ura4*$^{+}$/+ *leu1-32*/+ *ura4-D18/ura4-D18 ade6-M210/ade6-M216*
	6117	h$^{+/-}$ *nif1Δ::ura4*$^{+}$/*nif1Δ::ura4*$^{+}$ *leu1-32*/+ *ura4-D18/ura4-D18 ade6-M210/ade6-M216*
	4454	h$^{+/-}$ *nim1Δ::LEU2*/+ *pom1Δ::ura4*$^{+}$/+ *leu1-32/leu1-32 ura4-D18/ura4-D18 ade6-M210/ade6-M216*
	4684	h$^{+/-}$ *wee1Δ::ura4*$^{+}$/+ *leu1-32*/+ *ura4-D18/ura4-D18 ade6-M210/ade6-M216*
	6054	h$^{-/-}$ *wee1Δ::ura4*$^{+}$/+ *nim1Δ::LEU2*/+ *leu1-32/leu1-32 ura4-D18/ura4-D18 ade6-M210/ade6-M216*
	6113	h$^{+/-}$ *wee1Δ::ura4*$^{+}$/+ *pom1Δ::ura4*$^{+}$/+ *leu1-32*/+ *ura4-D18/ura4-D18 ade6-M210/ade6-M216*
	4640	h$^{+/-}$ 2x*act1*$^{+}$*::ura4*$^{+}$/+ (3x*act1*$^{+}$) *leu1-32*/+ *ura4-D18/ura4-D18 ade6-M210/ade6-M216*
	4651	h$^{+/-}$ *nim1Δ::LEU2*/+ 2x*act1*$^{+}$*::ura4*$^{+}$/+ (3x*act1*$^{+}$) *leu1-32*/*leu1-32 ura4-D18/ura4-D18 ade6-M210/ade6-M216*
	4658	h$^{+/-}$ *nim1Δ::LEU2*/*nim1Δ::LEU2* 2x*act1*$^{+}$*::ura4*$^{+}$/+ (3x*act1*$^{+}$) *leu1-32*/*leu1-32 ura4-D18/ura4-D18 ade6-M210/ade6-M216*
	4869	h$^{+/-}$ *pom1Δ::ura4*$^{+}$/+ 2x*act1*$^{+}$*::ura4*$^{+}$/+ (3x*act1*$^{+}$) *leu1-32*/+ *ura4-D18/ura4-D18 ade6-M210/ade6-M216*
	4457	h$^{+/-}$ *nim1Δ::LEU2*/ *nim1Δ::LEU2 pom1Δ::ura4*$^{+}$/+ *leu1-32/leu1-32 ura4-D18*/*ura4-D18 ade6-M210/ade6-M216*
	4962	h$^{+/-}$ *nim1Δ::LEU2*/*nim1Δ::LEU2* *pom1Δ::ura4*$^{+}$/*pom1Δ::ura4*$^{+}$ *leu1-32/leu1-32 ura4-D18*/*ura4-D18 ade6-M210/ade6-M216*

Figure 7	5335	h$^{+/-}$ *nim1Δ::LEU2/nim1Δ::LEU2 nif1Δ::ura4^{+}/nif1Δ::ura4^{+} leu1-32/leu1-32 ura4-D18/ura4-D18 ade6-M210/ade6-M216*
	4688	h$^{+/-}$ *wee1Δ::ura4^{+}/wee1Δ::ura4^{+} leu1-32/+ ura4-D18/ura4-D18 ade6-M210/ade6-M216*
	5469	h$^{+/-}$ *nif1Δ::ura4^{+}/nif1Δ::ura4^{+} wee1Δ::ura4^{+}/wee1Δ::ura4^{+} ura4-D18/ura4-D18 ade6-M210/ade6-M216*
	4693	h$^{+/-}$ *nim1Δ::LEU2/nim1Δ::LEU2 wee1Δ::ura4^{+}/wee1Δ::ura4^{+} leu1-32/leu1-32 ura4-D18/ura4-D18 ade6-M210/ade6-M216*
	5473	h$^{+/-}$ *nif1Δ::ura4^{+}/nif1Δ::ura4^{+} nim1Δ::LEU2/nim1Δ::LEU2 wee1Δ::ura4^{+}/wee1Δ::ura4^{+} leu1-32/leu1-32 ura4-D18/ura4-D18 ade6-M210/ade6-M216*
	5409	h$^{+/-}$ *cdc25-22/cdc25-22 wee1Δ::ura4^{+}/wee1Δ::ura4^{+} ura4-D18/ura4-D18 ade6-M210/ade6-M216*
	5388	h$^{+/-}$ *cdc25-22/cdc25-22 wee1Δ::ura4^{+}/wee1Δ::ura4^{+} nim1Δ::LEU2/nim1Δ::LEU2 leu1-32/leu1-32 ura4-D18/ura4-D18 ade6-M210/ade6-M216*
Figure 8	3174	h^{+} *lys1^{+}::GFP-wee1 wee1Δ::ura4^{+} ura4-D18*
	3507	h^{+} *pom1Δ::ura4^{+} lys1^{+}::GFP-wee1 wee1Δ::ura4-3233 ura4-D18*
	4542	h^{+} *nim1Δ::LEU2 lys1^{+}::GFP-wee1 wee1Δ::ura4^{+} leu1-32 ura4-D18 ade6-M210*
	4607	h^{+} *nim1Δ::LEU2 pom1Δ::ura4^{+} lys1^{+}::GFP-wee1 wee1Δ::ura4-3233 leu1-32 ura4-D18 ade6-M216*
	5452	h^{+} *nif1Δ::ura4^{+} lys1^{+}::GFP-wee1 wee1Δ::ura4-3233 ura4-D18 ade6-M210*
	3180	h$^{+/-}$ *lys1^{+}::GFP-wee1/lys1^{+}::GFP-wee1 wee1Δ::ura4^{+}/wee1Δ::ura4^{+} leu1-32/+ ura4-D18/ura4-D18 ade6-M210/ade6-M216*
	3526	h$^{+/-}$ *pom1Δ::ura4^{+}/pom1Δ::ura4^{+} lys1^{+}::GFP-wee1/lys1^{+}::GFP-wee1 wee1Δ::ura4-3233/wee1Δ::ura4-3233 ura4-D18/ura4-D18 ade6-M210/ade6-M216*

Figure 8	3529	h$^{+/-}$ *pom1Δ::ura4^{+}/+ lys1^{+}::GFP-wee1/lys1^{+}::GFP-wee1 wee1Δ::ura4-3233/wee1Δ::ura4-3233 ura4-D18/ura4-D18 ade6-M210/ade6-M216*
	5277	h$^{+/-}$ 2x*pom1^{+}::ura4^{+}*/2x*pom1^{+}::ura4^{+}* (4x*pom1^{+}*) *lys1^{+}::GFP-wee1/lys1^{+}::GFP-wee1 wee1Δ::ura4-3233/wee1Δ::ura4-3233 ura4-D18/ura4-D18 ade6-M210/ade6-M216*
	3673	h$^{+/-}$ *act1-ts/act1-ts pom1Δ::ura4^{+}/+ lys1^{+}::GFP-wee1/lys1^{+}::GFP-wee1 wee1Δ::ura4-3233/wee1Δ::ura4-3233 ura4-D18/ura4-D18 ade6-M210/ade6-M216*
	4574	h$^{+/-}$ *nim1Δ::LEU2/nim1Δ::LEU2 lys1^{+}::GFP-wee1/lys1^{+}::GFP-wee1 wee1Δ::ura4^{+}/wee1Δ::ura4-3233 leu1-32/leu1-32 ura4-D18/ura4-D18 ade6-M210/ade6-M216*
	4880	h$^{+/-}$ *adf1-1/adf1-1 nim1Δ::LEU2/nim1Δ::LEU2 lys1^{+}::GFP-wee1/lys1^{+}::GFP-wee1 wee1Δ::ura4^{+}/wee1Δ::ura4^{+} leu1-32/leu1-32 ura4-D18/ura4-D18 ade6-M210/ade6-M216*
	6126	h$^{+/-}$ *nim1Δ::LEU2/+ lys1^{+}::GFP-wee1/lys1^{+}::GFP-wee1 wee1Δ::ura4^{+}/wee1Δ::ura4-3233 leu1-32/leu1-32 ura4-D18/ura4-D18 ade6-M210/ade6-M216*
	4612	h+/- *nim1Δ::LEU2/nim1Δ::LEU2 pom1Δ::ura4^{+}/+ lys1^{+}::GFP-wee1/lys1^{+}::GFP-wee1 wee1Δ::ura4-3233/wee1Δ::ura4-3233 leu1-32/leu1-32 ura4-D18/ura4-D18 ade6-M210/ade6-M216*
	4554	h$^{+/-}$ *nim1Δ::LEU2/+ pom1Δ::ura4^{+}/+ lys1^{+}::GFP-wee1/lys1^{+}::GFP-wee1 wee1Δ::ura4-3233/wee1Δ::ura4-3233 leu1-32/leu1-32 ura4-D18/ura4-D18 ade6-M210/ade6-M216*
	5233	h$^{+/-}$ 2x*nim1^{+}::ura4^{+}*/2x*nim1^{+}::ura4^{+}* (4x*nim1^{+}*) *lys1^{+}::GFP-wee1/lys1^{+}::GFP-wee1 wee1Δ::ura4-3233/wee1Δ::ura4-3233 ura4-D18/ura4-D18 ade6-M210/ade6-M216*

Figure 8	5457	h$^{+/-}$ *nif1Δ::ura4*$^{+}$*/nif1Δ::ura4*$^{+}$ *lys1*$^{+}$*::GFP-wee1/lys1*$^{+}$*::GFP-wee1* *wee1Δ::ura4-3233/wee1Δ::ura4-3233* *ura4-D18/ura4-D18 ade6-M210/ade6-M216*
	5460	h$^{+/-}$ *nif1Δ::ura4*$^{+}$*/+ lys1*$^{+}$*::GFP-wee1/lys1*$^{+}$*::GFP-wee1* *wee1Δ::ura4-3233/wee1Δ::ura4-3233* *ura4-D18/ura4-D18 ade6-M210/ade6-M216*
	5502	h$^{+/-}$ *nif1Δ::ura4*$^{+}$*/nif1Δ::ura4*$^{+}$ *nim1Δ::LEU2/nim1Δ::LEU2* *lys1*$^{+}$*::GFP-wee1/lys1*$^{+}$*::GFP-wee1* *wee1Δ::ura4-3233/wee1Δ::ura4-3233 leu1-32/leu1-32* *ura4-D18/ura4-D18 ade6-M210/ade6-M216*
	4813	h$^{+/-}$ 2x*act1*$^{+}$*::ura4*$^{+}$*/+* (3x*act1*$^{+}$) *lys1*$^{+}$*::GFP-wee1/lys1*$^{+}$*::GFP-wee1* *wee1Δ::ura4-3233/wee1Δ::ura4-3233* *ura4-D18/ura4-D18 ade6-M210/ade6-M216*
	4816	h$^{+/-}$ 2x*act1*$^{+}$*::ura4*$^{+}$*/+* (3x*act1*$^{+}$) *pom1Δ::ura4*$^{+}$*/+* *lys1*$^{+}$*::GFP-wee1/lys1*$^{+}$*::GFP-wee1* *wee1Δ::ura4-3233/wee1Δ::ura4-3233* *ura4-D18/ura4-D18 ade6-M210/ade6-M216*
	4865	h$^{+/-}$ 2x*act1*$^{+}$*::ura4*$^{+}$*/+* (3x*act1*$^{+}$) *nim1Δ::LEU2/+* *lys1*$^{+}$*::GFP-wee1/lys1*$^{+}$*::GFP-wee1* *wee1Δ::ura4-3233/wee1Δ::ura4-3233 leu1-32/leu1-32* *ura4-D18/ura4-D18 ade6-M210/ade6-M216*
	5444	h$^{+/-}$ 2x*act1*$^{+}$*::ura4*$^{+}$*/+* (3x*act1*$^{+}$) 2x*pom1+::ura4*$^{+}$*/*2x*pom1*$^{+}$*::ura4*$^{+}$ (4x*pom1*$^{+}$) *lys1*$^{+}$*::GFP-wee1/lys1*$^{+}$*::GFP-wee1* *wee1Δ::ura4-3233/wee1Δ::ura4-3233* *ura4-D18/ura4-D18 ade6-M210/ade6-M216*
	5491	h$^{+/-}$ 2x*act1*$^{+}$*::ura4*$^{+}$*/+* (3x*act1*$^{+}$) 2x*nim1*$^{+}$*::ura4*$^{+}$*/*2x*nim1*$^{+}$*::ura4*$^{+}$ (4x*nim1*$^{+}$) *lys1*$^{+}$*::GFP-wee1/lys1*$^{+}$*::GFP-wee1* *wee1Δ::ura4-3233/wee1Δ::ura4-3233* *ura4-D18/ura4-D18 ade6-M210/ade6-M216*

Figure 8	5567	h$^{+/-}$ 2x*act1^{+}::ura4^{+}*/+ (3x*act1^{+}*) *nif1Δ::ura4^{+}/nif1Δ::ura4^{+} lys1^{+}::GFP-wee1/lys1^{+}::GFP-wee1 wee1Δ::ura4-3233/wee1Δ::ura4-3233 ura4-D18/ura4-D18 ade6-M210/ade6-M216*
	5563	h$^{+/-}$ 2x*act1^{+}::ura4^{+}*/+ (3x*act1^{+}*) *nif1Δ::ura4^{+}/+ lys1^{+}::GFP-wee1/lys1^{+}::GFP-wee1 wee1Δ::ura4-3233/wee1Δ::ura4-3233 ura4-D18/ura4-D18 ade6-M210/ade6-M216*
Figure 9	2829	h$^{+/-}$ *ade6-M210/ade6-M216*
	5646	h$^{-/-}$ *cdc25Δ::ura4^{+}*/+ *leu1-32*/+ *ura4-D18/ura4-D18 ade6-M210/ade6-M216*
	6136	h$^{+/-}$ *nim1Δ::LEU2*/+ *leu1-32/leu1-32 ade6-M210/ade6-M216*
	6146	h$^{+/-}$ *cdc25Δ::ura4^{+}*/+ *nim1Δ::LEU2*/+ *leu1-32/leu1-32 ura4-D18*/+ (or -/-) *ade6-M210/ade6-M216*
	6057	h$^{-/-}$ *pom1Δ::ura4^{+}*/+ *leu1-32*/+ *ura4-D18/ura4-D18 ade6-M210/ade6-M216*
	6145	h$^{+/-}$ *cdc25Δ::ura4^{+}*/+ *pom1Δ::ura4^{+}*/+ *leu1-32*/+ (or +/+) *ura4-D18/ura4-D18 ade6-M210/ade6-M216*
Figure 10	1345	h^{-} *cps8-188* (*act1-ts*)
	3991	h^{-} *act1-ts wee1-50*
	3660	h$^{+/-}$ *act1-ts*/*act1-ts ade6-M210/ade6-M216*
	4068	h$^{+/-}$ *act1-ts*/*act1-ts wee1-50*/*wee1-50 leu1-32*/+ *ade6-M210/ade6-M216*
	3797	h$^{+/-}$ *cdc25-22*/*cdc25-22 wee1-50*/*wee1-50 ade6-M210/ade6-M216*
	1701	h$^{+/-}$ *act1-ts*/*act1-ts cdc25-22*/*cdc25-22 wee1-50*/*wee1-50 ade6-M210/ade6-M216*
	3872	h$^{+/-}$ *act1-ts*/*act1-ts cdc25-22*/*cdc25-22 wee1-50*/*wee1-50 pom1Δ::ura4^{+}*/+ *leu1-32*/+ *ura4-D18/ura4-D18 ade6-M210/ade6-M216*
	5681	h$^{+/-}$ *act1-ts*/*act1-ts cdc25-22*/*cdc25-22 wee1-50*/*wee1-50 pom1Δ::ura4^{+}*/+ *nim1Δ::LEU2/nim1Δ::LEU2 leu1-32*/*leu1-32 ura4-D18/ura4-D18 ade6-M210/ade6-M216*

Figure 10	4684	h$^{+/-}$ *wee1Δ::ura4^{+}/+ leu1-32/+ ura4-D18/ura4-D18 ade6-M210/ade6-M216*
	5669	h$^{-/-}$ *act1Δ::ura4^{+}/+ wee1Δ::ura4^{+}/+ leu1-32/+ ura4-D18/ura4-D18 ade6-M210/ade6-M216*
	6054	h$^{-/-}$ *wee1Δ::ura4^{+}/+ nim1Δ::LEU2/+ leu1-32/leu1-32 ura4-D18/ura4-D18 ade6-M210/ade6-M216*
	6096	h$^{+/-}$ *act1Δ::ura4^{+}/+ wee1Δ::ura4^{+}/+ nim1Δ::LEU2/+ leu1-32/leu1-32 ura4-D18/ura4-D18 ade6-M210/ade6-M216*
	1407	h$^{+/-}$ *lys1^{+}::GFP-wee1/lys1^{+}::GFP-wee1 wee1Δ::ura4^{+}/wee1Δ::ura4^{+} leu1-32/leu1-32 ura4-D18/ura4-D18 ade6-M210/ade6-M216*
	1621	h$^{+/-}$ *act1-ts/act1-ts lys1^{+}::GFP-wee1/lys1^{+}::GFP-wee1 wee1Δ::ura4^{+}/wee1Δ::ura4^{+} leu1-32/leu1-32 ura4-D18/ura4-D18 ade6-M210/ade6-M216*
	4734	h$^{+/-}$ *adf1-1/adf1-1 lys1^{+}::GFP-wee1/lys1^{+}::GFP-wee1 wee1Δ::ura4^{+}/wee1Δ::ura4^{+} ura4-D18/ura4-D18 ade6-M210/ade6-M216*
	4854	h$^{+/-}$ *act1-ts/act1-ts adf1-1/adf1-1 lys1^{+}::GFP-wee1/lys1^{+}::GFP-wee1 wee1Δ::ura4^{+}/wee1Δ::ura4^{+} ura4-D18/ura4-D18 ade6-M210/ade6-M216*
	2548	h$^{+/-}$ *lys1^{+}::GFP-NESx2-wee1/lys1^{+}::GFP-NESx2-wee1 wee1Δ::ura4^{+}/wee1Δ::ura4^{+} leu1-32/leu1-32 ura4-D18/ura4-D18 ade6-M210/ade6-M216*
	6129	h$^{+/-}$ *act1-ts/act1-ts lys1^{+}::GFP-NESx2-wee1/lys1^{+}::GFP-NESx2-wee1 wee1Δ::ura4^{+}/wee1Δ::ura4^{+} leu1-32/leu1-32 ura4-D18/ura4-D18 ade6-M210/ade6-M216*
	4775	h$^{+/-}$ *adf1-1/adf1-1 lys1^{+}::GFP-NESx2-wee1/lys1^{+}::GFP-NESx2-wee1 wee1Δ::ura4^{+}/wee1Δ::ura4^{+} ura4-D18/ura4-D18*
	4944	h$^{+/-}$ *act1-ts/act1-ts adf1-1/adf1-1 lys1^{+}::GFP-NESx2-wee1/lys1^{+}::GFP-NESx2-wee1 wee1Δ::ura4^{+}/wee1Δ::ura4^{+} ura4-D18/ura4-D18 ade6-M210/ade6-M216*

Figure 11	2802	h$^-$ wild
	4149	h$^-$ 2x*cdc13$^+$::ura4+ ura4-D18*
	4133	h$^-$ 2x*cdc25$^+$::ura4$^+$ ura4-D18*
	4507	h$^-$ 2x*pom1$^+$::ura4$^+$ ura4-D18*
	4123	h$^-$ 2x*act1$^+$::ura4$^+$ ura4-D18*
	3432	h$^-$ *lys1$^+$::GFP-wee1*
	3174	h$^+$ *lys1$^+$::GFP-wee1 wee1Δ::ura4$^+$ ura4-D18*
	4222	h$^{+/-}$ *lys1$^+$::GFP-wee1/lys1-131 wee1Δ::ura4-3233/+ leu1-32/+ ura4-D18/+ ade6-M210/ade6-M216*
	4742	h$^-$ 2x*act1$^+$::ura4$^+$* 2x*pom1$^+$::ura4$^+$* 2x*cdc13$^+$::ura4$^+$* 2x*cdc25$^+$::ura4$^+$ lys1$^+$::GFP-wee1 ura4-D18*
	4745	h$^+$ 2x*act1$^+$::ura4$^+$* 2x*pom1$^+$::ura4$^+$* 2x*cdc13$^+$::ura4$^+$* 2x*cdc25$^+$::ura4$^+$ lys1$^+$::GFP-NESx2-wee1 ura4-D18*
	4247	h$^-$ 2x*act1$^+$::ura4$^+$* 2x*cdc13$^+$::ura4$^+$* 2x*cdc25$^+$::ura4$^+$ lys1$^+$::GFP-wee1 ura4-D18*
	4750	h$^-$ 2x*pom1$^+$::ura4$^+$* 2x*cdc13$^+$::ura4$^+$* 2x*cdc25$^+$::ura4$^+$ lys1$^+$::GFP-wee1 ura4-D18*
	4467	h$^-$ 2x*act1$^+$::ura4$^+$* 2x*pom1$^+$::ura4$^+$* 2x*cdc13$^+$::ura4$^+$ lys1$^+$::GFP-wee1 ura4-D18*
	4461	h$^-$ 2x*act1$^+$::ura4$^+$* 2x*pom1$^+$::ura4$^+$* 2x*cdc25$^+$::ura4$^+$ lys1$^+$::GFP-wee1 ura4-D18*
	5215	h$^+$ 2x*nim1$^+$::ura4$^+$* 2x*act1$^+$::ura4$^+$* 2x*cdc13$^+$::ura4$^+$* 2x*cdc25$^+$::ura4$^+$ lys1$^+$::GFP-wee1 ura4-D18*
	5168	h$^-$ 2x*nim1$^+$::ura4$^+$* 2x*pom1$^+$::ura4$^+$* 2x*act1$^+$::ura4$^+$* 2x*cdc13$^+$::ura4$^+$* 2x*cdc25$^+$::ura4$^+$ lys1$^+$::GFP-wee1 ura4-D18*
	4249	h$^-$ 2x*act1$^+$::ura4$^+$* 2x*cdc13$^+$::ura4$^+$* 2x*cdc25$^+$::ura4$^+$ lys1$^+$::GFP-NESx2-wee1 ura4-D18*
	5184	h$^-$ 2x*nim1$^+$::ura4$^+$* 2x*act1$^+$::ura4$^+$* 2x*cdc13$^+$::ura4$^+$* 2x*cdc25$^+$::ura4$^+$ lys1$^+$::GFP-NESx2-wee1 ura4-D18*
	4217	h$^-$ 2x*cdc13$^+$::ura4$^+$* 2x*cdc25$^+$::ura4$^+$ lys1$^+$::GFP-wee1 ura4-D18*
	5126	h$^-$ 2x*nim1$^+$::ura4$^+$* 2x*cdc13$^+$::ura4$^+$* 2x*cdc25$^+$::ura4$^+$ lys1$^+$::GFP-wee1 ura4-D18*
	4213	h$^-$ 2x*act1$^+$::ura4$^+$* 2x*cdc13$^+$::ura4$^+$ lys1$^+$::GFP-wee1 ura4-D18*

Figure 11	5115	h$^-$ 2x*nim1$^+$::ura4$^+$* 2x*act1$^+$::ura4$^+$* 2x*cdc13$^+$::ura4$^+$ lys1$^+$::GFP-wee1 ura4-D18*
	4208	h$^-$ 2x*act1$^+$::ura4$^+$* 2x*cdc25$^+$::ura4$^+$ lys1$^+$::GFP-wee1 ura4-D18*
	5112	h$^-$ 2x*nim1$^+$::ura4$^+$* 2x*act1$^+$::ura4$^+$* 2x*cdc25$^+$::ura4$^+$ lys1$^+$::GFP-wee1 ura4-D18*
Supplemental Figure 1	1579	h$^+$ *cdc25Δ::ura4$^+$::cdc25-GFP::leu1$^+$ leu1-32 ura4-D18*
	1286	h$^-$ *cdc25-22 leu1-32 ura4-D18 ade6-M216*
	1845	h$^+$ *cdc13-117 cdc25Δ::ura4$^+$::cdc25-GFP::leu1$^+$ leu1-32 ura4-D18 ade6-M210*
	1289	h$^-$ *wee1-50 leu1-32 ura4-D18*
	2266	h$^-$ 2x*act1$^+$::ura4$^+$ leu1-32 ura4-D18 ade6-M210*
	3351	h$^{-/-}$ *cdc25Δ::ura4$^+$::cdc25-GFP::leu1$^+$/ cdc25Δ::ura4$^+$::cdc25-GFP::leu1$^+$ leu1-32/leu1-32 ura4-D18/ura4-D18*
	2148	h$^{+/-}$ *act1Δ::ura4$^+$/+ cdc25Δ::ura4-2012::cdc25-GFP::leu1$^+$/ cdc25Δ::ura4-2012::cdc25-GFP::leu1$^+$ leu1-32/leu1-32 ura4-D18/ura4-D18 ade6-M210/ade6-M216*
Supplemental Figure 2	3174	h$^+$ *lys1$^+$::GFP-wee1 wee1Δ::ura4$^+$ ura4-D18*
	3180	h$^{+/-}$ *lys1$^+$::GFP-wee1/lys1$^+$::GFP-wee1 wee1Δ::ura4$^+$/wee1Δ::ura4$^+$ leu1-32/+ ura4-D18/ura4-D18 ade6-M210/ade6-M216*
	1461	h$^-$ *cdc25Δ::ura4$^+$::cdc25-GFP::leu1$^+$ leu1-32 ura4-D18*
	3614	h$^{-/-}$ *cdc25Δ::ura4$^+$::cdc25-GFP::leu1$^+$/ cdc25Δ::ura4$^+$::cdc25-GFP::leu1$^+$ leu1-32/leu1-32 ura4-D18/ura4-D18 ade6-M210/ade6-M216*
Supplemental Figure 3	3180	h$^{+/-}$ *lys1$^+$::GFP-wee1/lys1$^+$::GFP-wee1 wee1Δ::ura4$^+$/wee1Δ::ura4$^+$ leu1-32/+ ura4-D18/ura4-D18 ade6-M210/ade6-M216*
	3256	h$^{+/-}$ *cdc2-3w/cdc2-3w lys1$^+$::GFP-wee1/lys1$^+$::GFP-wee1 wee1Δ::ura4$^+$/wee1Δ::ura4$^+$ ura4-D18/ura4-D18 ade6-M210/ade6-M216*

Supplemental Figure 3	3212	h$^{+/-}$ *lys1^{+}::GFP-NESx2-wee1/lys1^{+}::GFP-NESx2-wee1 wee1Δ::ura4^{+}/wee1Δ::ura4^{+} leu1-32/+ ura4-D18/ura4-D18 ade6-M210/ade6-M216*
	3260	h$^{+/-}$ *cdc2-3w/cdc2-3w lys1^{+}::GFP-NESx2-wee1/lys1^{+}::GFP-NESx2-wee1 wee1Δ::ura4^{+}/wee1Δ::ura4^{+} ura4-D18/ura4-D18 ade6-M210/ade6-M216*
Supplemental Figure 4	YEY132	h^{+} *cdc25Δ::ura4^{+}::cdc25-GFP::leu1^{+} leu1-32 ura4-D18*
	YHO182	h^{-} *cdc25Δ::ura4^{+}::cdc25-NLS-GFP::leu1^{+} leu1-32 ura4-D18*
Supplemental Figure 5	3180	h$^{+/-}$ *lys1^{+}::GFP-wee1/lys1^{+}::GFP-wee1 wee1Δ::ura4^{+}/wee1Δ::ura4^{+} leu1-32/+ ura4-D18/ura4-D18 ade6-M210/ade6-M216*
	3322	h$^{+/-}$ *act1Δ::ura4^{+}/+ lys1^{+}::GFP-wee1/lys1^{+}::GFP-wee1 wee1Δ::ura4-3233/wee1Δ::ura4-3233 leu1-32/+ ura4-D18/ura4-D18 ade6-M210/ade6-M216*
	3529	h$^{+/-}$ *pom1Δ::ura4^{+}/+ lys1^{+}::GFP-wee1/lys1^{+}::GFP-wee1 wee1Δ::ura4-3233/wee1Δ::ura4-3233 ura4-D18/ura4-D18 ade6-M210/ade6-M216*
	3212	h$^{+/-}$ *lys1^{+}::GFP-NESx2-wee1/lys1^{+}::GFP-NESx2-wee1 wee1Δ::ura4^{+}/wee1Δ::ura4^{+} leu1-32/+ ura4-D18/ura4-D18 ade6-M210/ade6-M216*
	3325	h$^{+/+}$ *act1Δ::ura4^{+}/+ lys1^{+}::GFP-NESx2-wee1/lys1^{+}::GFP-NESx2-wee1 wee1Δ::ura4-3233/wee1Δ::ura4-3233 leu1-32/+ ura4-D18/ura4-D18 ade6-M210/ade6-M216*
	3533	h$^{+/-}$ *pom1Δ::ura4^{+}/+ lys1^{+}::GFP-NESx2-wee1/lys1^{+}::GFP-NESx2-wee1 wee1Δ::ura4-3233/wee1Δ::ura4-3233 ura4-D18/ura4-D18 ade6-M210/ade6-M216*
Supplemental Figure 6	2802	h^{-} wild
	1345	h^{-} *cps8-188* (*act1-ts*)
	3823	h^{-} *cdc25-22*
	1664	h^{-} *act1-ts cdc25-22*
	3967	h^{-} *wee1-50*
	3991	h^{-} *act1-ts wee1-50*

Supplemental Figure 6	3760	h^- *cdc25-22 wee1-50*
	1689	h^- *cdc25-22 wee1-50 act1-ts ade6-M216*
	2829	$h^{+/-}$ *ade6-M210/ade6-M216*
	3660	$h^{+/-}$ *act1-ts/act1-ts ade6-M210/ade6-M216*
	3691	$h^{+/-}$ *cdc25-22/cdc25-22 ade6-M210/ade6-M216*
	3677	$h^{+/-}$ *act1-ts/act1-ts cdc25-22/cdc25-22 ade6-M210/ade6-M216*
	4031	$h^{+/-}$ *wee1-50/wee1-50 leu1-32/+ ade6-M210/ade6-M216*
	4068	$h^{+/-}$ *act1-ts/act1-ts wee1-50/wee1-50 leu1-32/+ ade6-M210/ade6-M216*
	3797	$h^{+/-}$ *cdc25-22/cdc25-22 wee1-50/wee1-50 ade6-M210/ade6-M216*
	1701	$h^{+/-}$ *act1-ts/act1-ts cdc25-22/cdc25-22 wee1-50/wee1-50 ade6-M210/ade6-M216*

Figure 1.

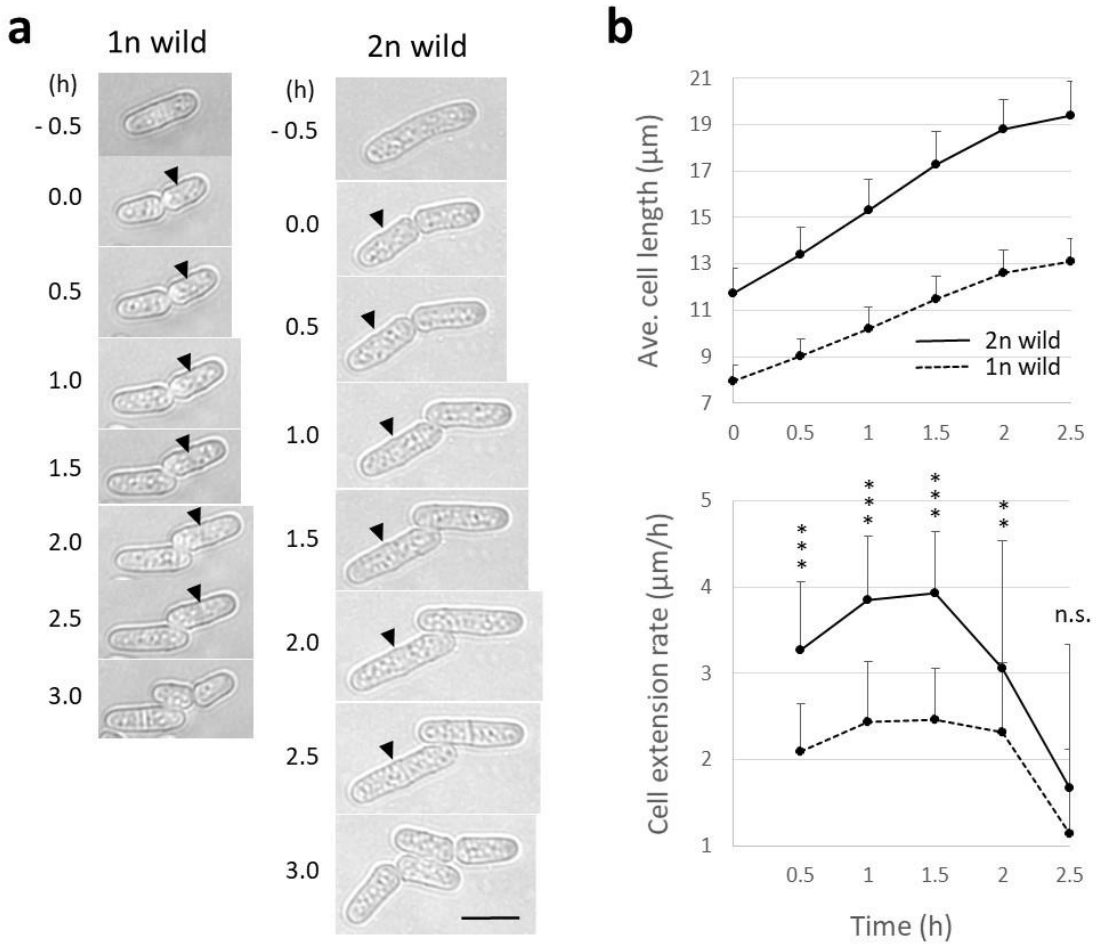
a
1n wild
2n wild
(h)
- 0.5
0.0
0.5
1.0
1.5
2.0
2.5
3.0
b
Ave. cell length (μm)
2n wild
1n wild
Cell extension rate (μm/h)
***
***
***
**
n.s.
Time (h)

Figure 2.

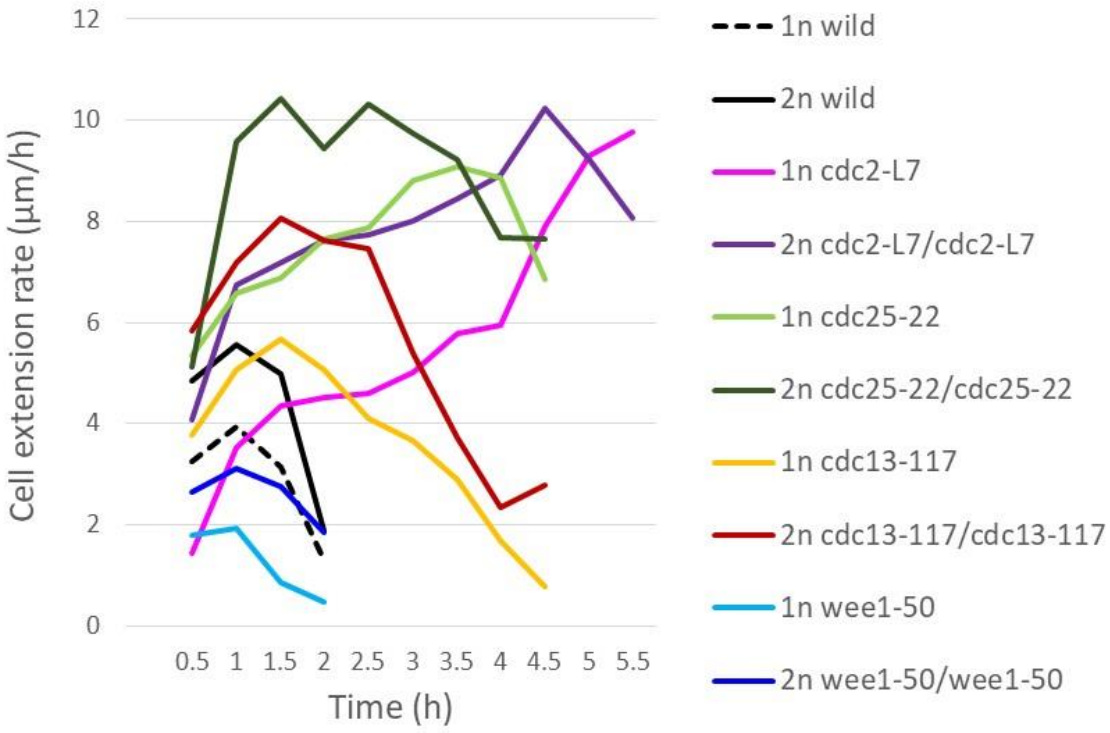
Cell extension rate (µm/h)
12
10
8
6
4
2
0
0.5 1 1.5 2 2.5 3 3.5 4 4.5 5 5.5
Time (h)
1n wild
2n wild
1n cdc2-L7
2n cdc2-L7/cdc2-L7
1n cdc25-22
2n cdc25-22/cdc25-22
1n cdc13-117
2n cdc13-117/cdc13-117
1n wee1-50
2n wee1-50/wee1-50

Figure 3.

a

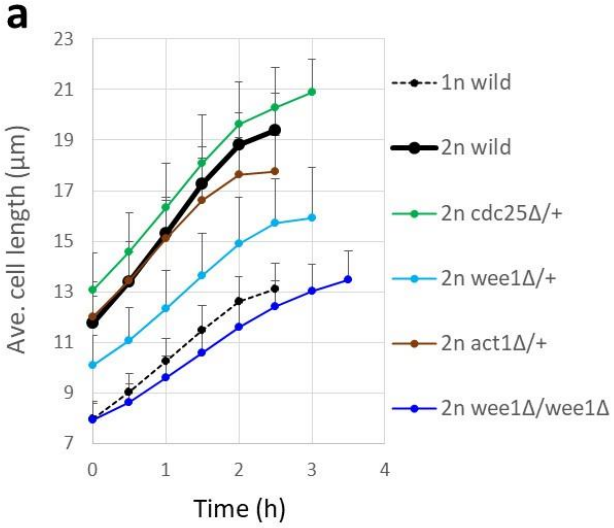

b

Genotype	CER (Max)	*p* value					
2n wild	3.94±0.71	—					
2n *wee1Δ*/+	2.66±0.66	***	—				
2n *cdc25Δ*/+	3.57±0.95	*		—		n.s.	
2n *act1Δ*/+	3.33±0.84	***			—	n.s.	
2n *wee1Δ*/+ *cdc25Δ*/+	2.75±0.87	***	n.s.	***			***
2n *wee1Δ*/+ *act1Δ*/+	2.98±0.81	***	*		*		*
2n *cdc25Δ*/+ *act1Δ*/+	3.47±1.0	*				—	n.s.
2n *wee1Δ*/+ *cdc25Δ*/+ *act1Δ*/+	3.43±0.81	**					—
2n *wee1Δ*/*wee1Δ*	2.08±0.58	***	***				
1n wild	2.47±0.59	***	n.s.				

c

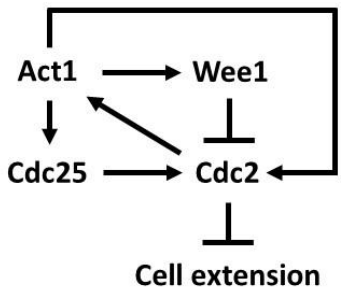

Figure 4.

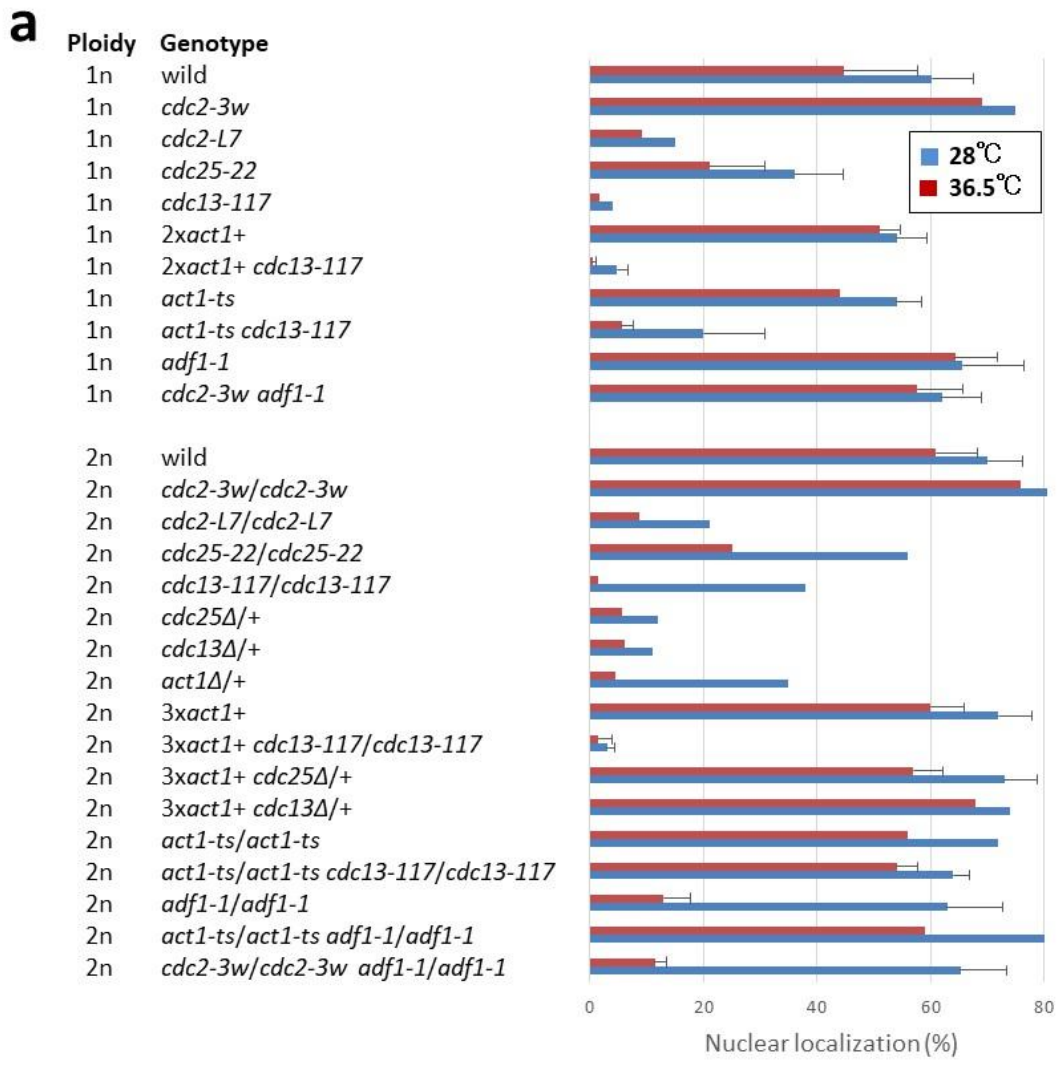
a
Ploidy
Genotype
1n wild
1n cdc2-3w
1n cdc2-L7
1n cdc25-22
1n cdc13-117
1n 2xact1+
1n 2xact1+ cdc13-117
1n act1-ts
1n act1-ts cdc13-117
1n adf1-1
1n cdc2-3w adf1-1
2n wild
2n cdc2-3w/cdc2-3w
2n cdc2-L7/cdc2-L7
2n cdc25-22/cdc25-22
2n cdc13-117/cdc13-117
2n cdc25Δ/+
2n cdc13Δ/+
2n act1Δ/+
2n 3xact1+
2n 3xact1+ cdc13-117/cdc13-117
2n 3xact1+ cdc25Δ/+
2n 3xact1+ cdc13Δ/+
2n act1-ts/act1-ts
2n act1-ts/act1-ts cdc13-117/cdc13-117
2n adf1-1/adf1-1
2n act1-ts/act1-ts adf1-1/adf1-1
2n cdc2-3w/cdc2-3w adf1-1/adf1-1
28℃
36.5℃
0
20
40
60
80
Nuclear localization (%)

Figure 4. (continued)

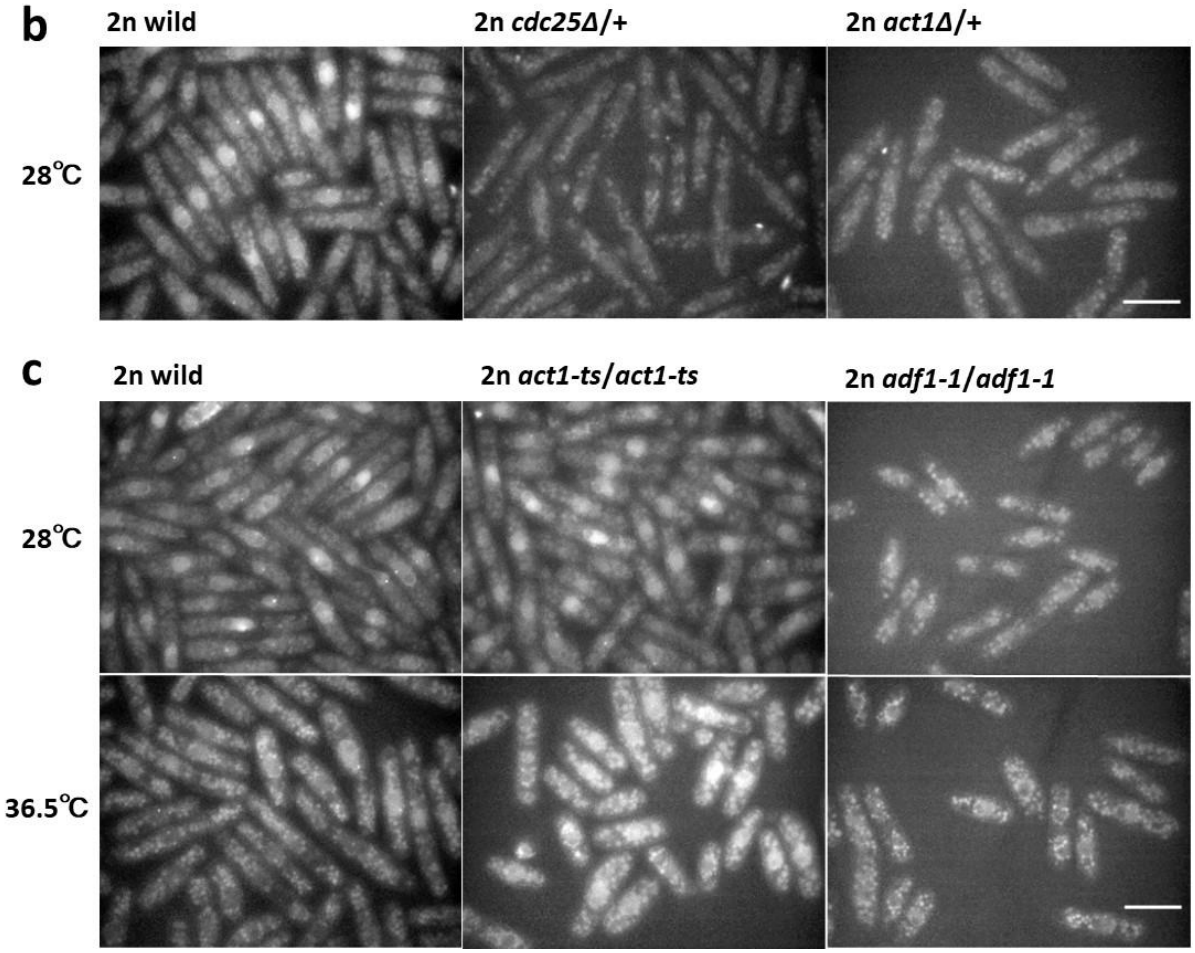

Figure 5.

a

Ploidy	*cdc25-GFP*	*act1*	*adf1*	*wee1*	*cdc13*
1n	+	+	+	+	+
1n	+	-	+	+	+
1n	+	+	-	+	+
1n	+	+	+	-	+
1n	+	+	+	+	-
1n	+	-	+	+	-
1n	+	+	-	+	-
1n	*NLS*	+	+	+	+
1n	*NLS*	+	+	-	+
1n	*NLS*	-	+	+	+
1n	*NLS*	+	-	+	+

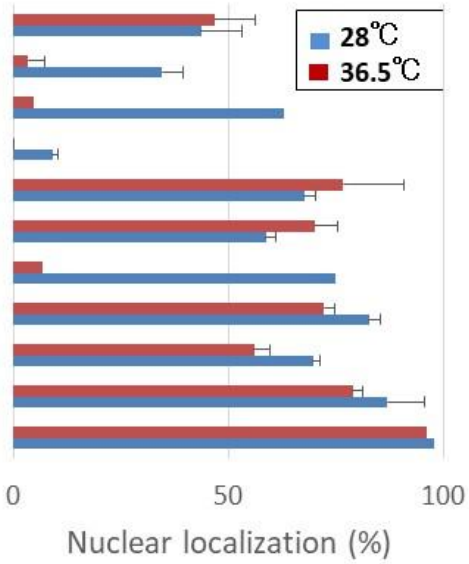

Ploidy	*cdc25-GFP*	*act1*	*adf1*	*wee1*	*cdc13*
2n	+/+	+/+	+/+	+/+	+/+
2n	+/+	-/-	+/+	+/+	+/+
2n	+/+	+/+	-/-	+/+	+/+
2n	+/+	+/+	+/+	-/-	+/+
2n	+/+	+/+	+/+	+/+	-/-
2n	+/+	-/-	+/+	+/+	-/-
2n	+/+	+/+	-/-	+/+	-/-
2n	+/+	+/+	+/+	+/Δ	+/+
2n	+/+	+/Δ	+/+	+/+	+/+
2n	+/+	+/Δ	+/+	+/Δ	+/+
2n	*NLS/NLS*	+/+	+/+	+/+	+/+
2n	*NLS/NLS*	+/+	+/+	-/-	+/+
2n	*NLS/NLS*	-/-	+/+	+/+	+/+
2n	*NLS/NLS*	+/+	-/-	+/+	+/+
2n	*NLS/NLS*	+/+	+/+	+/Δ	+/+

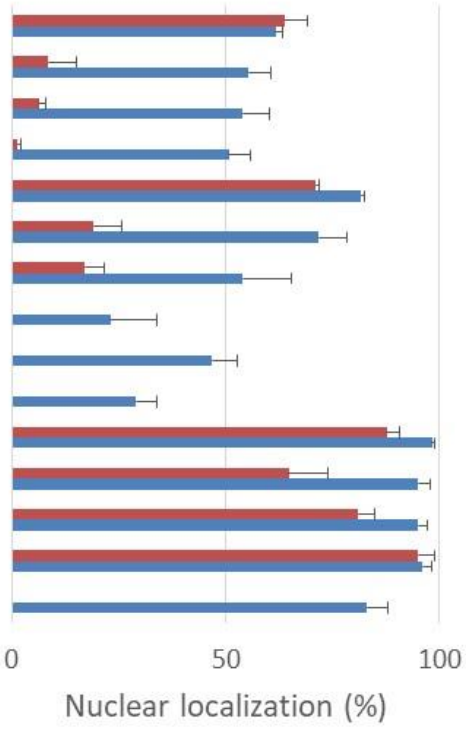

Figure 5. (continued)

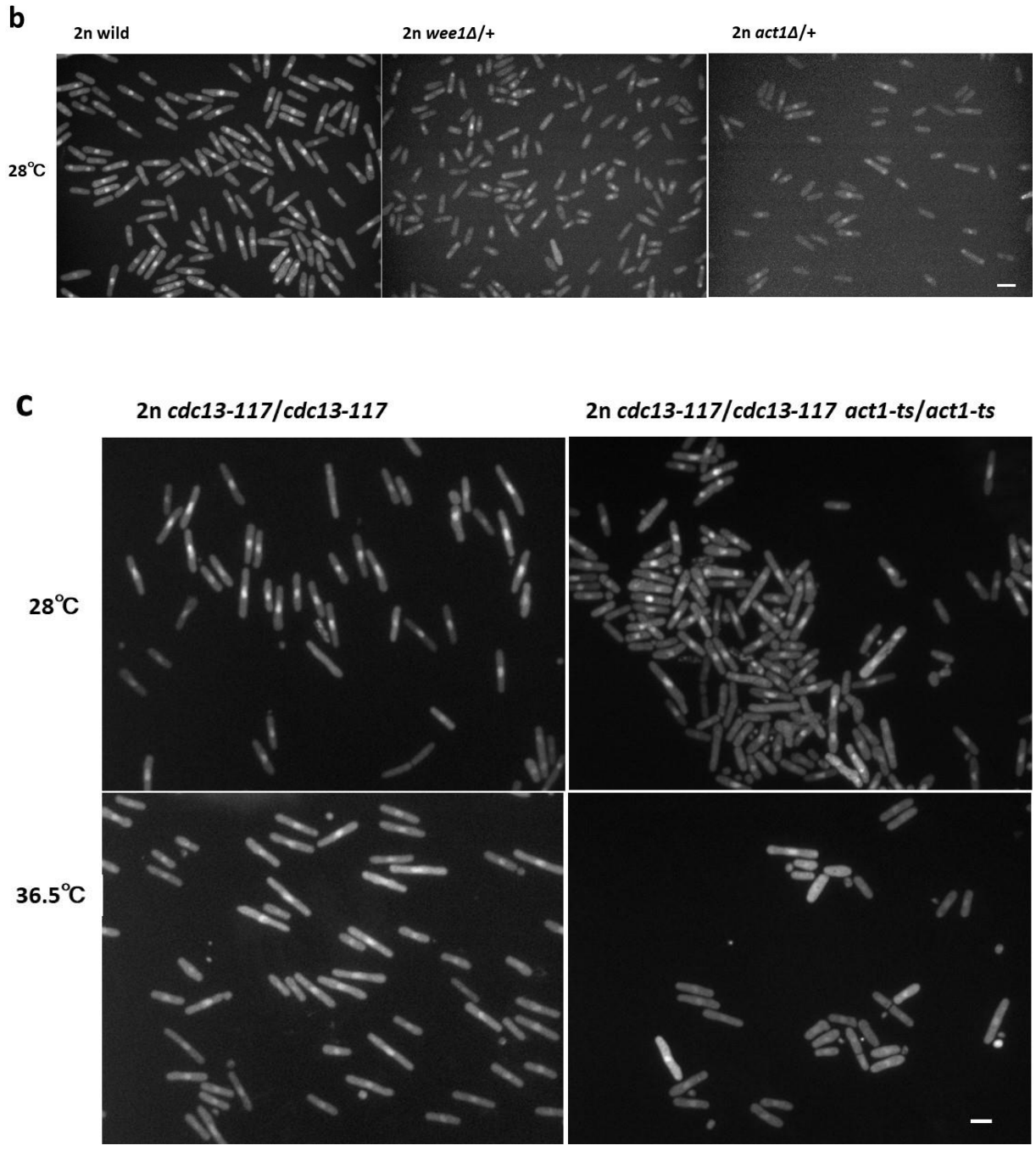

Figure 6.

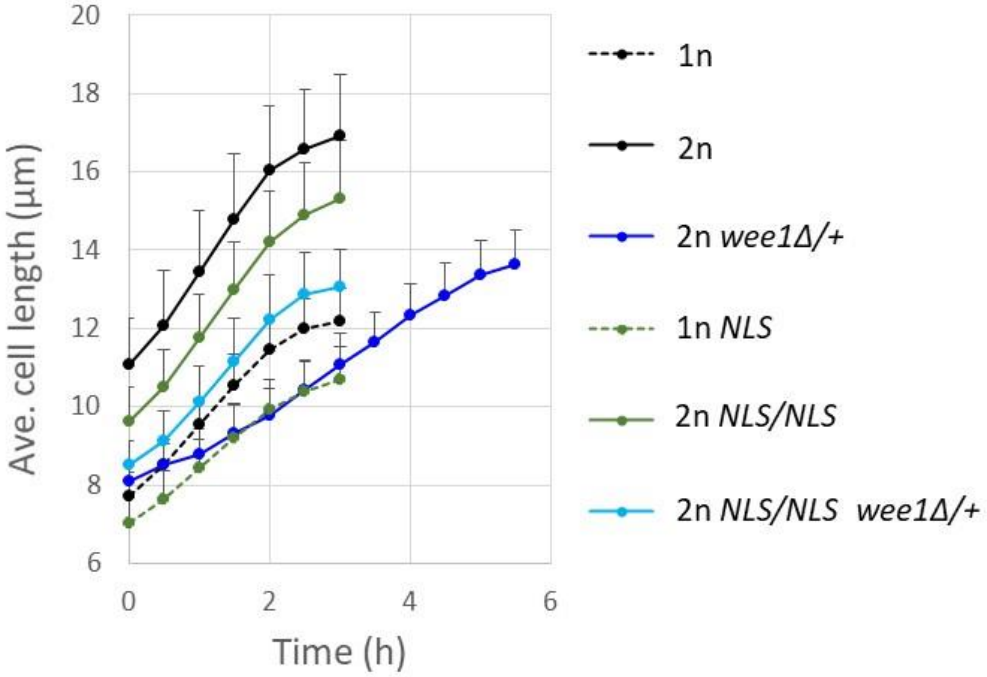

Genotype	CER (max)	P value			
1n *cdc25-GFP*	2.02±0.67	***			—
2n *cdc25-GFP/cdc25-GFP*	2.71±0.76	—			
2n *wee1Δ/+ cdc25-GFP/cdc25-GFP*	1.38±0.83	***		—	
1n *cdc25-NLS*	1.57±0.47		***		
2n *cdc25-NLS/cdc25-NLS*	2.50±0.74		—		
2n *wee1Δ/+ cdc25-NLS/cdc25-NLS*	2.09±0.63		*	***	n.s.

Figure 7.

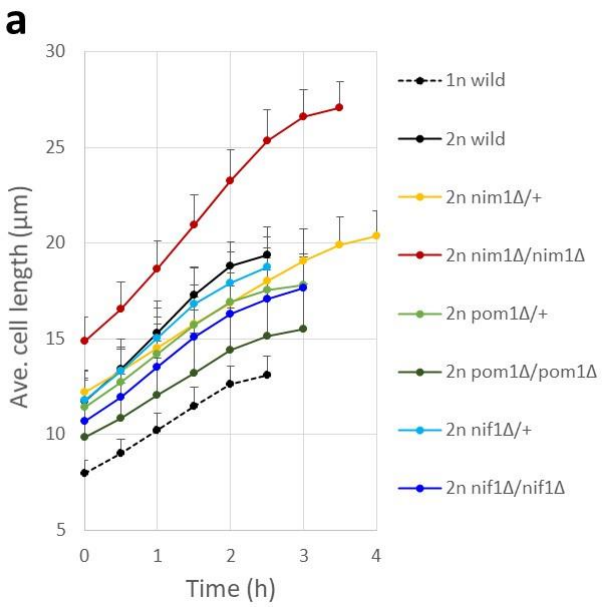

Genotype	CER (max)	P value				
2n wild	3.94 ± 0.71	—				
2n *nim1Δ/+*	2.54 ± 0.87	***	—			
2n *nim1Δ/nim1Δ*	4.62 ± 0.80	***				—
2n *pom1Δ/+*	3.02 ± 0.86	***				
2n *pom1Δ/pom1Δ*	2.38 ± 0.89	***				
2n *nif1Δ/+*	3.49 ± 0.92	*				
2n *nif1Δ/nif1Δ*	3.16 ± 0.79	***				
1n wild	2.47 ± 0.59	***	n.s.			
2n *nim1Δ/+ pom1Δ/+*	3.36 ± 1.38		**			
2n *wee1Δ/+*	2.66 ± 0.66			—		
2n *wee1Δ/+ nim1Δ/+*	2.42 ± 0.73			n.s.		
2n *wee1Δ/+ pom1Δ/+*	2.82 ± 0.81			n.s.		
2n 3x*act1+*	3.17 ± 0.80				—	
2n 3x*act1+ nim1Δ/+*	3.54 ± 1.39				n.s.	
2n 3x*act1+ nim1Δ/nim1Δ*	3.95 ± 1.02				***	
2n 3x*act1+ pom1Δ/+*	3.04 ± 0.83				n.s.	
2n *nim1Δ/nim1Δ pom1Δ/+*	4.51 ± 1.19					n.s.
2n *nim1Δ/nim1Δ pom1Δ/pom1Δ*	3.37 ± 0.82					***
2n *nim1Δ/nim1Δ nif1Δ/nif1Δ*	4.18 ± 0.87					*

Figure 7. (continued)

b

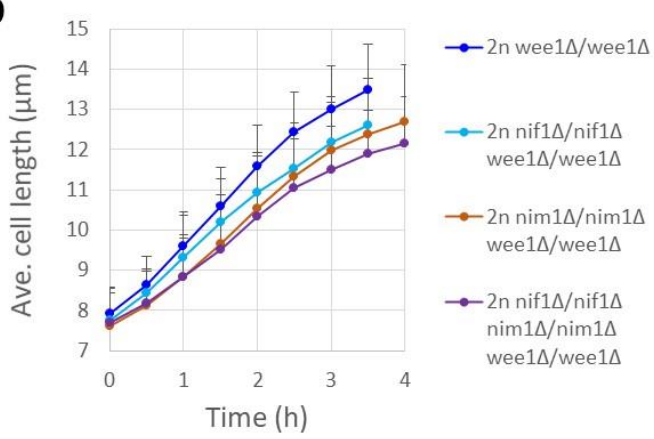

Genotype	CER (max)	P value
2n *wee1Δ/wee1Δ*	2.08 ± 0.58	—
2n *wee1Δ/wee1Δ nif1Δ/nif1Δ*	1.77 ± 0.50	*
2n *wee1Δ/wee1Δ nim1Δ/nim1Δ*	1.76 ± 0.81	*
2n *wee1Δ/wee1Δ nif1Δ/nif1Δ nim1Δ/nim1Δ*	1.63 ± 0.69	**

c

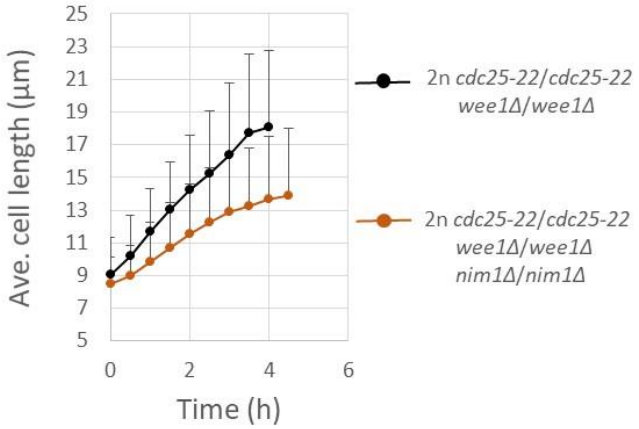

Genotype	CER (max)	P value
2n *cdc25-22/cdc25-22 wee1Δ/wee1Δ*	2.92 ± 1.14	—
2n *cdc25-22/cdc25-22 wee1Δ/wee1Δ nim1Δ/nim1Δ*	1.78 ± 1.37	***

Figure 8.

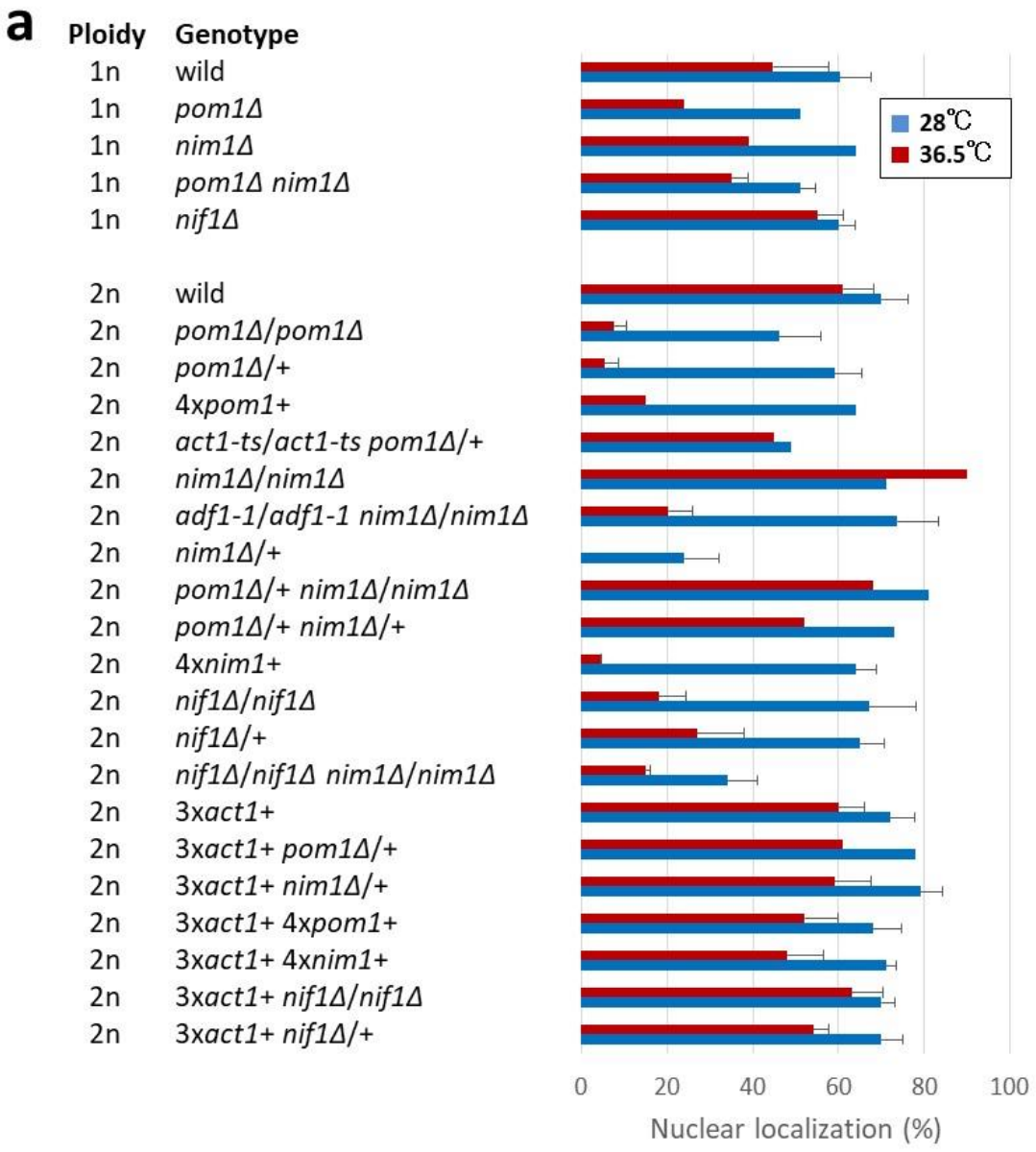
a
Ploidy
Genotype
1n wild
1n pom1Δ
1n nim1Δ
1n pom1Δ nim1Δ
1n nif1Δ
2n wild
2n pom1Δ/pom1Δ
2n pom1Δ/+
2n 4xpom1+
2n act1-ts/act1-ts pom1Δ/+
2n nim1Δ/nim1Δ
2n adf1-1/adf1-1 nim1Δ/nim1Δ
2n nim1Δ/+
2n pom1Δ/+ nim1Δ/nim1Δ
2n pom1Δ/+ nim1Δ/+
2n 4xnim1+
2n nif1Δ/nif1Δ
2n nif1Δ/+
2n nif1Δ/nif1Δ nim1Δ/nim1Δ
2n 3xact1+
2n 3xact1+ pom1Δ/+
2n 3xact1+ nim1Δ/+
2n 3xact1+ 4xpom1+
2n 3xact1+ 4xnim1+
2n 3xact1+ nif1Δ/nif1Δ
2n 3xact1+ nif1Δ/+
28℃
36.5℃
0
20
40
60
80
100
Nuclear localization (%)

Figure 8. (continued)

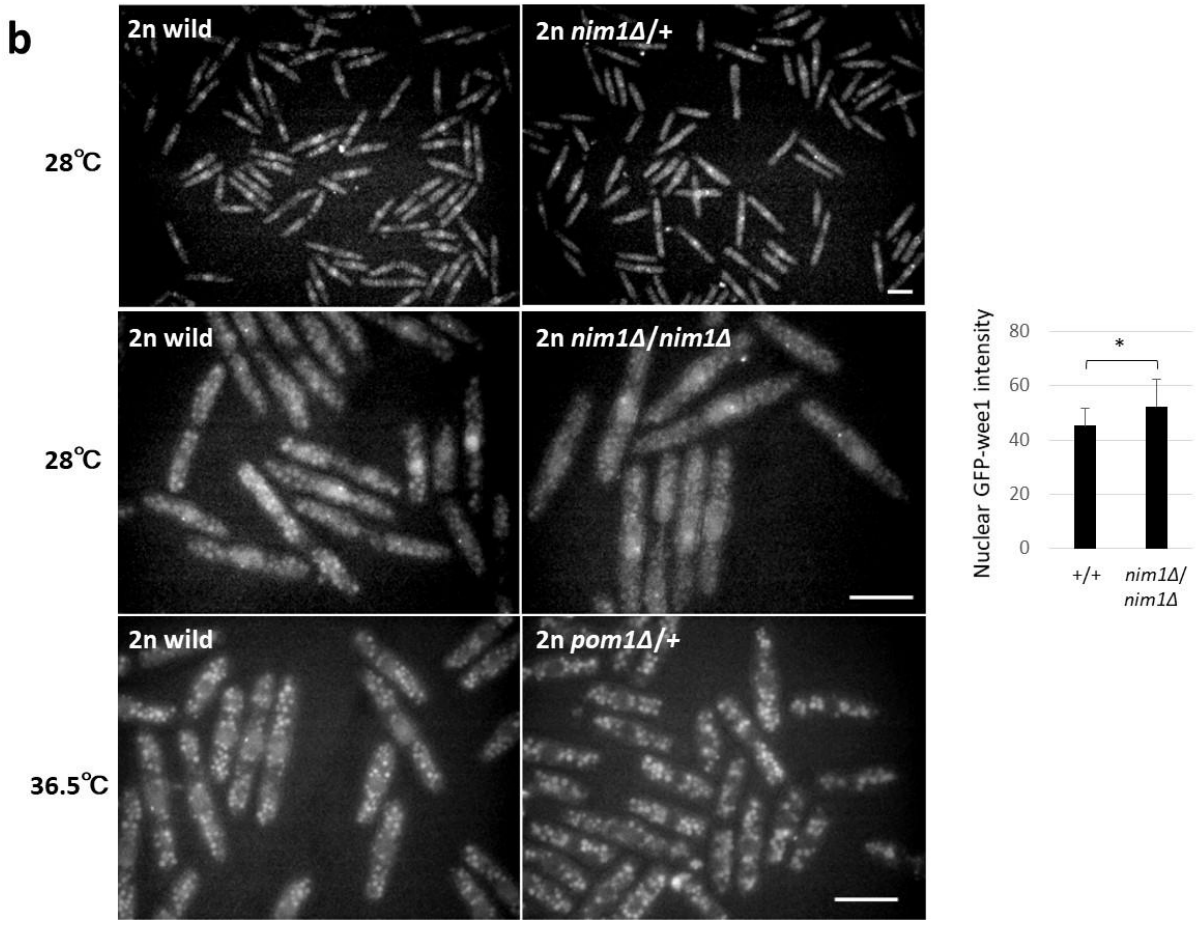

Figure 9.

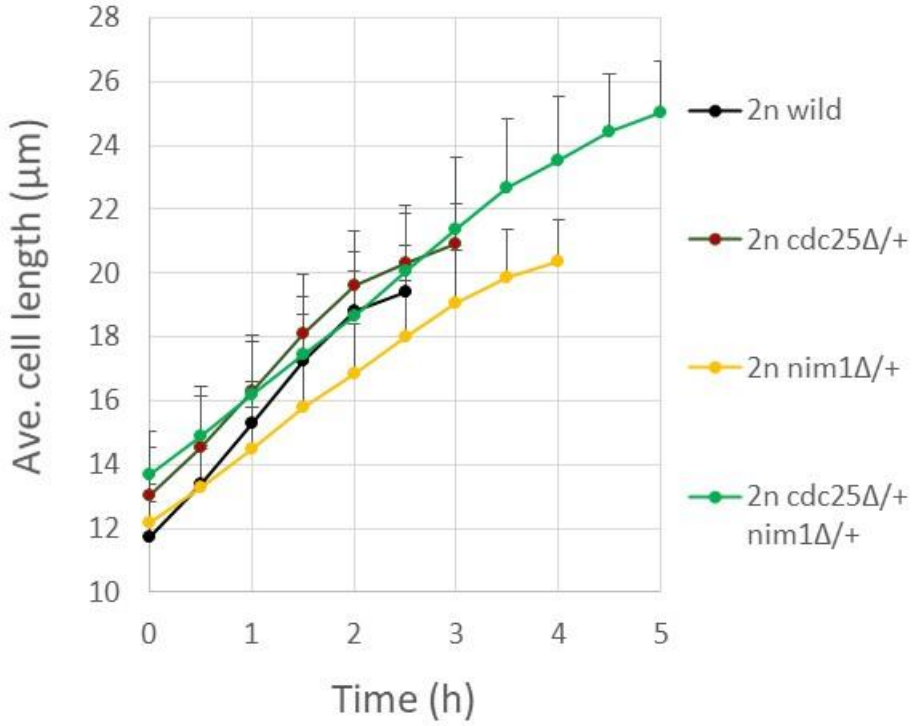

Genotype	CER (max)	P value		
2n *cdc25Δ/+*	3.57 ± 0.95	—		
2n *nim1Δ/+*	2.54 ± 0.87		—	
2n *pom1Δ/+*	3.02 ± 0.86			—
2n *cdc25Δ/+ nim1Δ/+*	2.78 ± 0.89	***	n.s.	
2n *cdc25Δ/+ pom1Δ/+*	3.89 ± 0.98	n.s.		***
2n wild	3.94 ± 0.71	*	***	***

Figure 10.

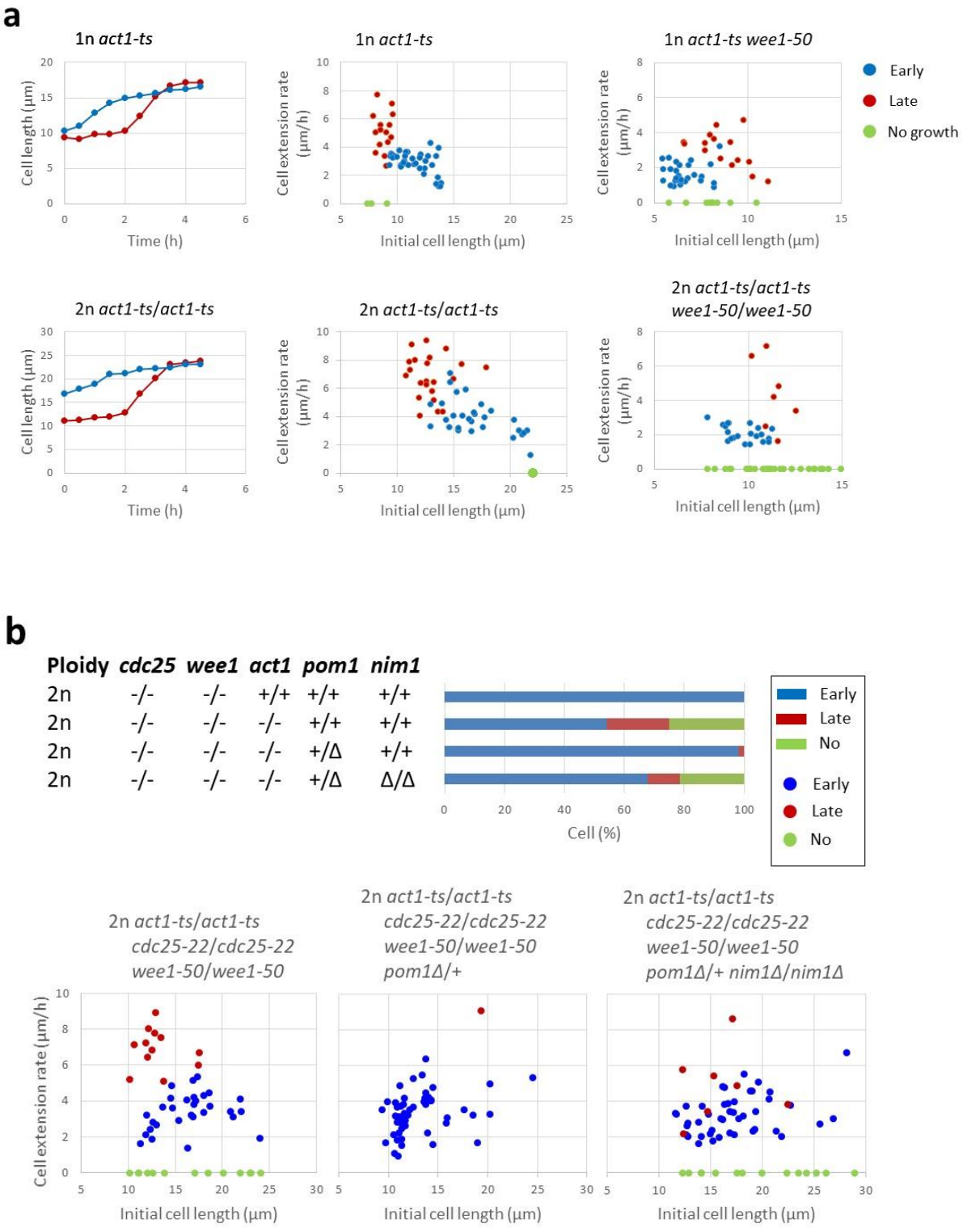
a
1n act1-ts
Cell length (µm)
Time (h)
1n act1-ts
Cell extension rate (µm/h)
Initial cell length (µm)
1n act1-ts wee1-50
Cell extension rate (µm/h)
Initial cell length (µm)
Early
Late
No growth
2n act1-ts/act1-ts
Cell length (µm)
Time (h)
2n act1-ts/act1-ts
Cell extension rate (µm/h)
Initial cell length (µm)
2n act1-ts/act1-ts wee1-50/wee1-50
Cell extension rate (µm/h)
Initial cell length (µm)
b
Ploidy cdc25 wee1 act1 pom1 nim1
2n -/- -/- +/+ +/+ +/+
2n -/- -/- -/- +/+ +/+
2n -/- -/- -/- +/Δ +/+
2n -/- -/- -/- +/Δ Δ/Δ
Cell (%)
Early
Late
No
Early
Late
No
2n act1-ts/act1-ts cdc25-22/cdc25-22 wee1-50/wee1-50
2n act1-ts/act1-ts cdc25-22/cdc25-22 wee1-50/wee1-50 pom1Δ/+
2n act1-ts/act1-ts cdc25-22/cdc25-22 wee1-50/wee1-50 pom1Δ/+ nim1Δ/nim1Δ
Cell extension rate (µm/h)
Initial cell length (µm)
Initial cell length (µm)
Initial cell length (µm)

Figure 10. (continued)

c

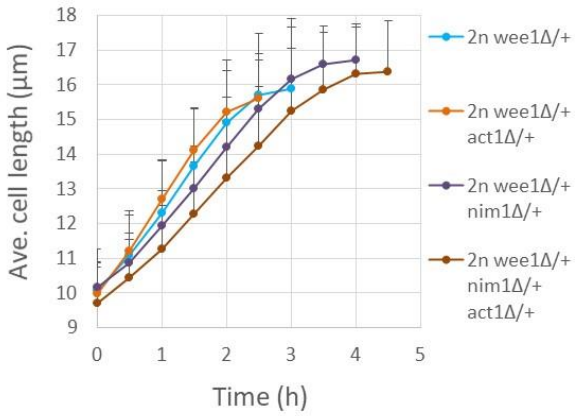

Genotype	CER (max)	P value	
2n *wee1Δ/+*	2.66±0.66	—	
2n *wee1Δ/+ act1Δ/+*	2.98±0.81	*	***
2n *wee1Δ/+ nim1Δ/+*	2.42±0.73	n.s.	*
2n *wee1Δ/+ nim1Δ/+ act1Δ/+*	2.08±0.80		—

d

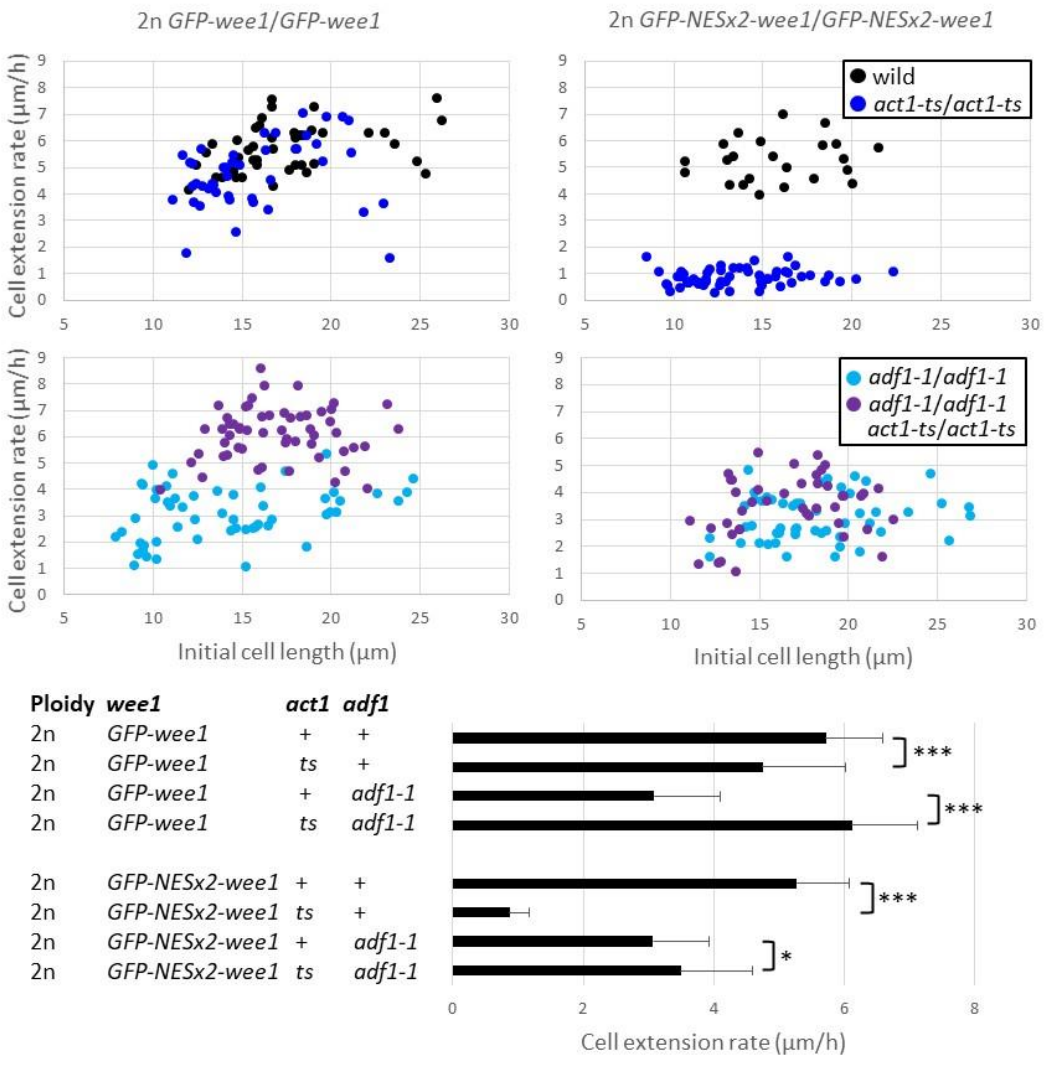

Figure 11.

a

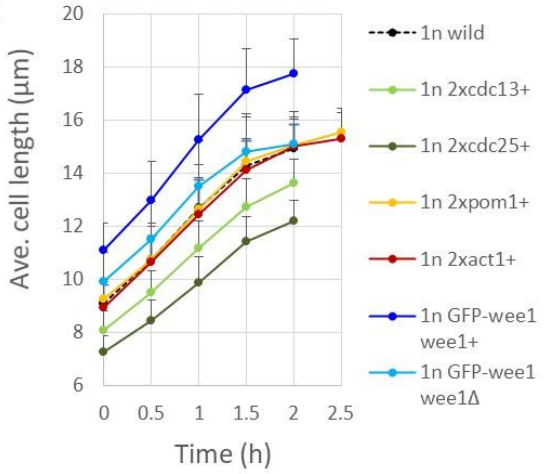

Genotype	CER (max)	P value	
1n wild	3.95 ± 0.77	—	
1n *GFP-wee1 wee1+*	4.57 ± 0.90	**	—
1n *GFP-wee1 wee1Δ*	4.02 ± 1.01	n.s.	*
1n 2x*pom1+*	3.85 ± 0.92	n.s.	
1n 2x*act1+*	3.63 ± 0.77	*	
1n 2x*cdc13+*	3.39 ± 0.72	***	
1n 2x*cdc25+*	3.05 ± 0.88	***	

b

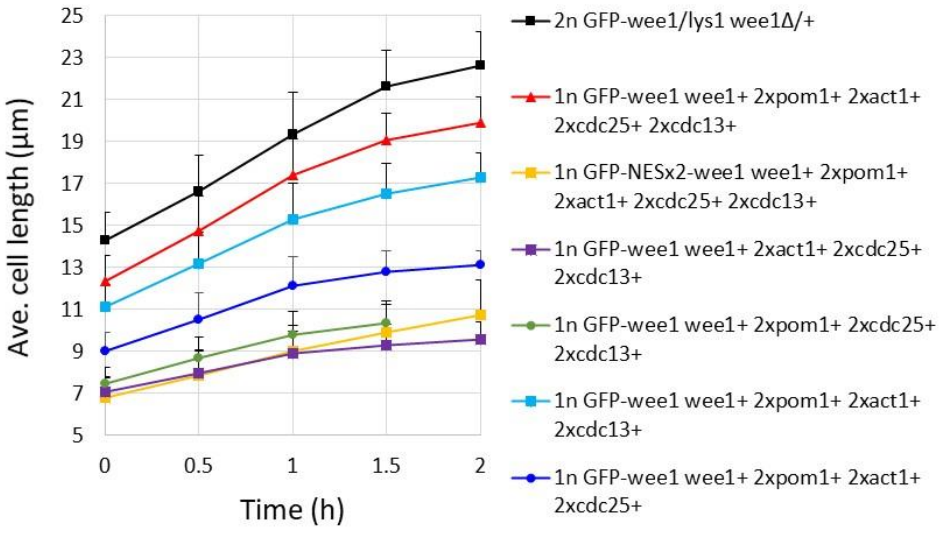

Genotype	CER (max)	P value
2n control	5.43 ± 1.49	n.s.
1n Complete	5.30 ± 1.06	—
1n NES	2.34 ± 0.90	***
1n − *pom1+*	1.85 ± 0.96	***
1n − *act1+*	2.40 ± 0.99	***
1n − *cdc25+*	4.29 ± 1.48	***
1n − *cdc13+*	3.27 ± 1.20	***

Figure 11. (continued)

C

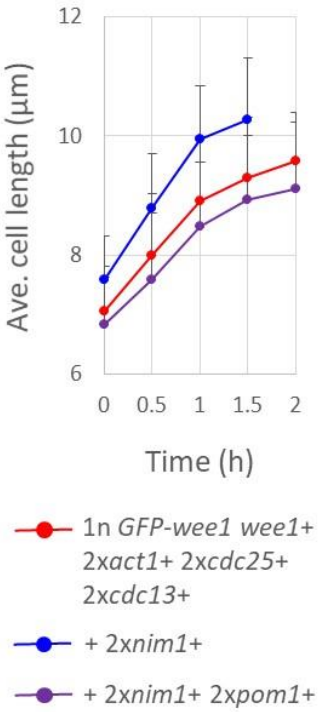

Genotype	CER (max)	P value
1n *GFP-wee1 wee1+ 2xact1+ 2xcdc25+ 2xcdc13+*	1.85±0.96	—
+ 2x*nim1+*	2.39±0.82	*
+ 2x*nim1+* 2x*pom1+*	1.88±0.98	n.s.
1n *GFP-NESx2-wee1 wee1+ 2xact1+ 2xcdc25+ 2xcdc13+*	2.50±1.06	—
+ 2x*nim1+*	2.01±0.95	*
1n *GFP-wee1 wee1+ 2xcdc25+ 2xcdc13+*	2.46±0.86	—
+ 2x*nim1+*	2.12±0.76	*
1n *GFP-wee1 wee1+ 2xact1+ 2xcdc13+*	4.03±0.97	—
+ 2x*nim1+*	3.39±0.98	**
1n *GFP-wee1 wee1+ 2xact1+ 2xcdc25+*	3.63±0.82	—
+ 2x*nim1+*	3.23±0.90	*

Figure 12.

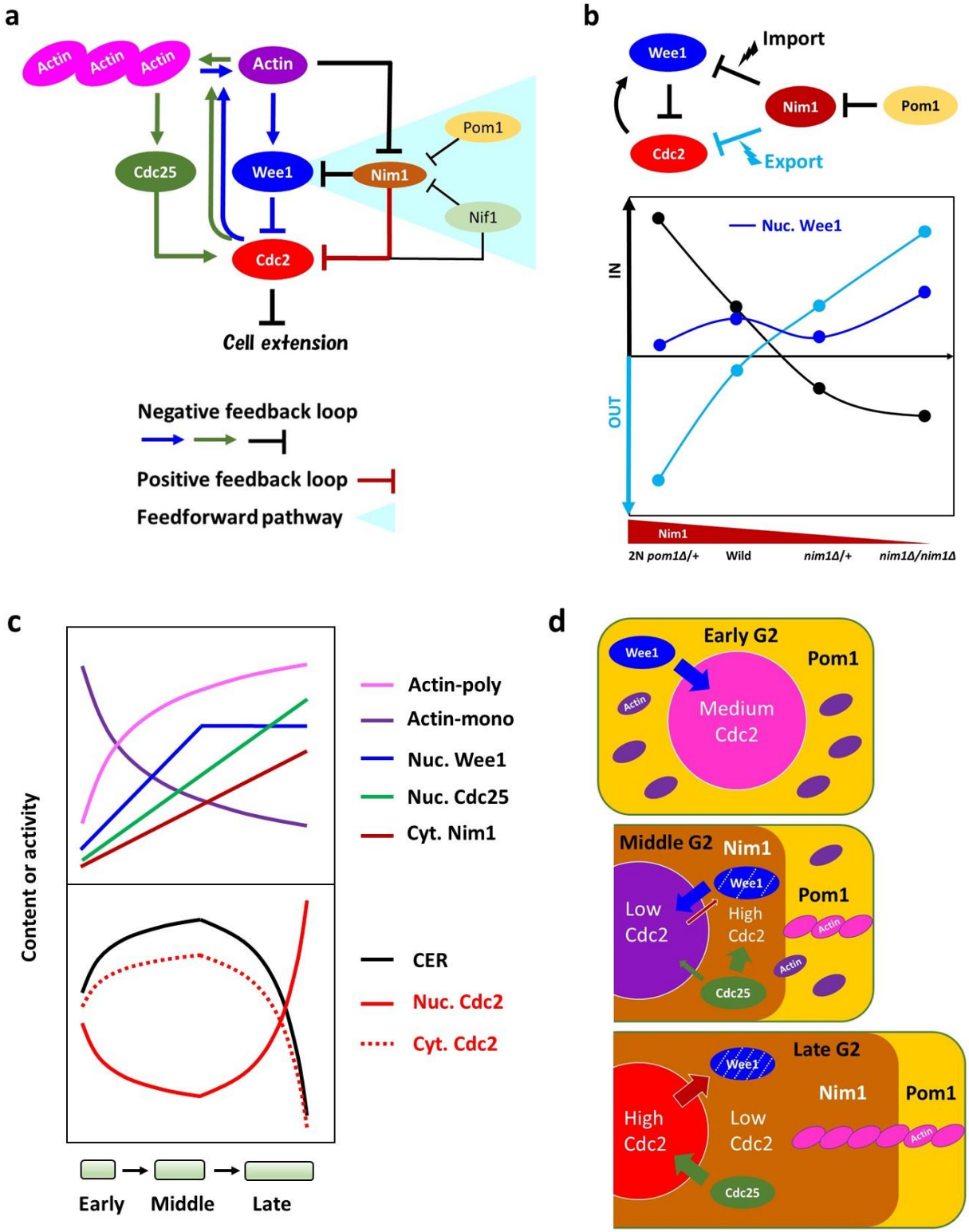
a
Actin
Actin
Actin
Actin
Cdc25
Wee1
Nim1
Pom1
Nif1
Cdc2
Cell extension
Negative feedback loop
Positive feedback loop
Feedforward pathway
b
Wee1
Import
Nim1
Pom1
Cdc2
Export
Nuc. Wee1
IN
OUT
Nim1
2N pom1Δ/+
Wild
nim1Δ/+
nim1Δ/nim1Δ
c
Content or activity
Actin-poly
Actin-mono
Nuc. Wee1
Nuc. Cdc25
Cyt. Nim1
CER
Nuc. Cdc2
Cyt. Cdc2
Early
Middle
Late
d
Early G2
Wee1
Pom1
Actin
Medium
Cdc2
Middle G2
Nim1
Wee1
Pom1
Low
Cdc2
High
Cdc2
Actin
Actin
Cdc25
Late G2
Wee1
Nim1
Pom1
High
Cdc2
Low
Cdc2
Actin
Cdc25

Supplemental Figure 1.

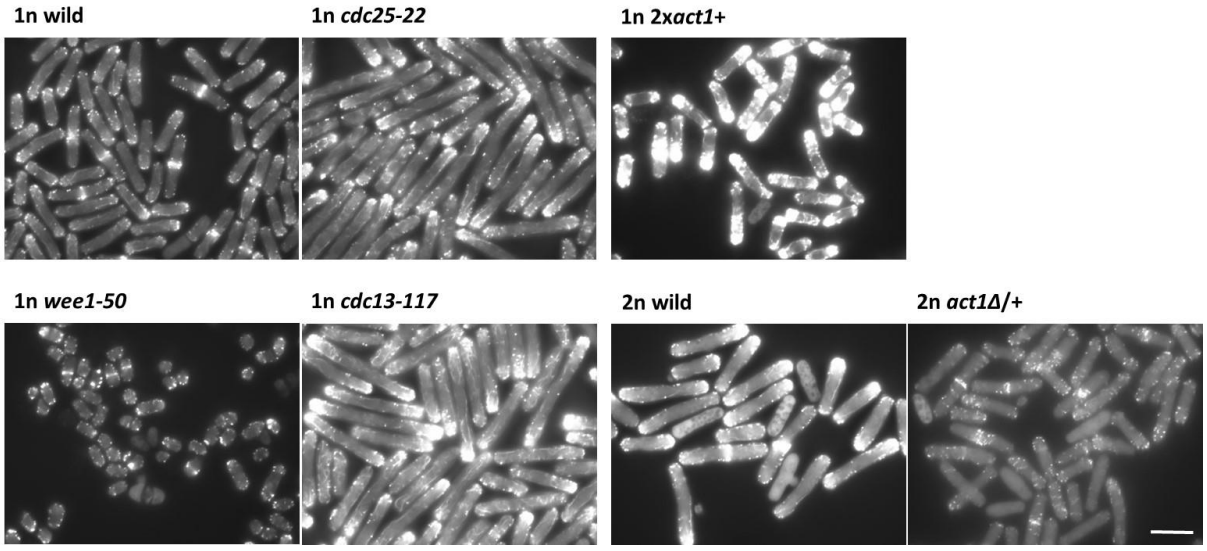

Supplemental Figure 2.

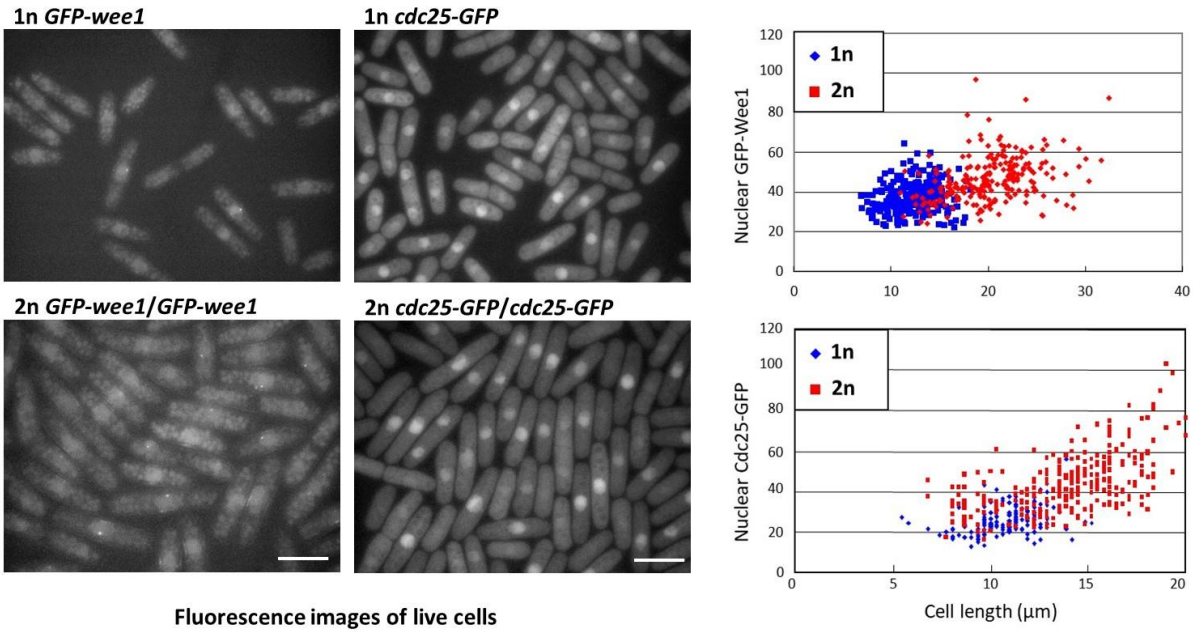

Supplemental Figure 3.

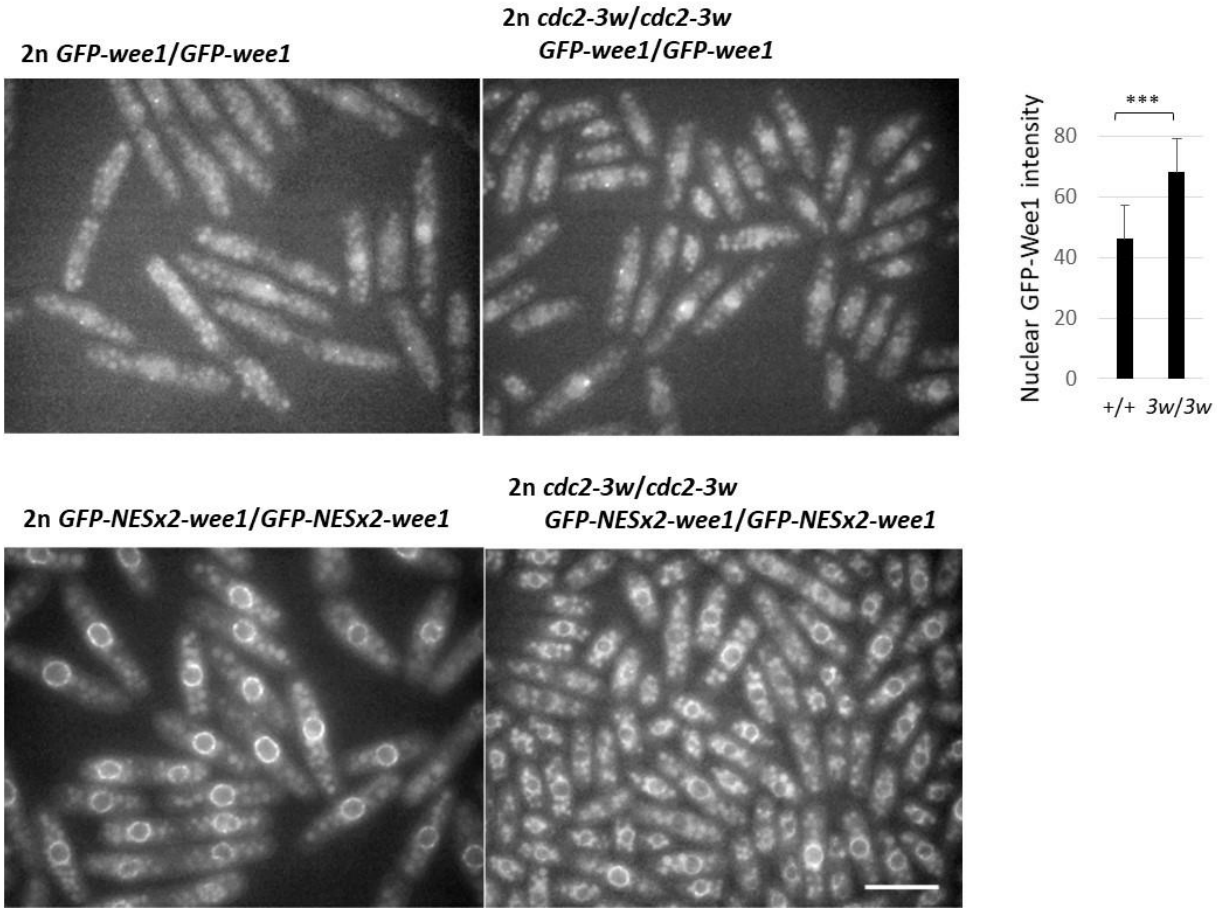

Supplemental Figure 4.

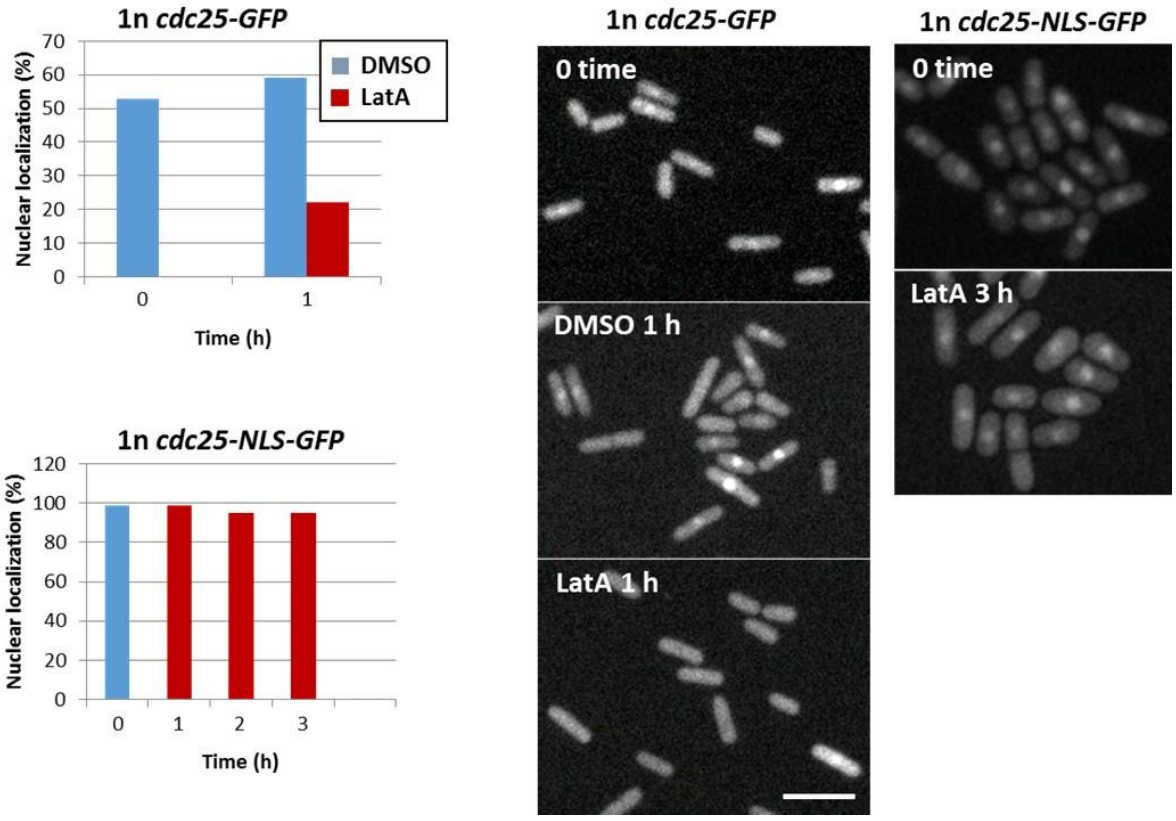

Supplemental Figure 5.

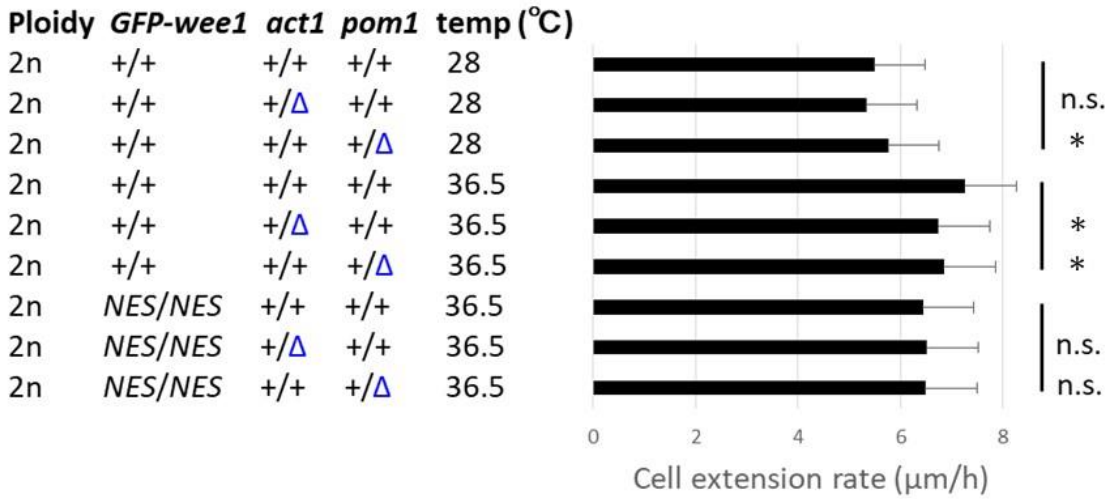

Supplemental Figure 6.